

USER'S GUIDE

Vapor Intrusion Estimation Tool for Unsaturated-Zone
Contaminant Sources

ESTCP Project ER-201125

JANUARY 2016

C.D. Johnson
M.J. Truex
M. Oostrom
Pacific Northwest National Laboratory

K.C. Carroll
New Mexico State University

A.K. Rice
Colorado School of Mines

Distribution Statement A
This document has been cleared for public release



Page Intentionally Left Blank

This report was prepared under contract to the Department of Defense Environmental Security Technology Certification Program (ESTCP). The publication of this report does not indicate endorsement by the Department of Defense, nor should the contents be construed as reflecting the official policy or position of the Department of Defense. Reference herein to any specific commercial product, process, or service by trade name, trademark, manufacturer, or otherwise, does not necessarily constitute or imply its endorsement, recommendation, or favoring by the Department of Defense.

Page Intentionally Left Blank

REPORT DOCUMENTATION PAGE

*Form Approved
OMB No. 0704-0188*

The public reporting burden for this collection of information is estimated to average 1 hour per response, including the time for reviewing instructions, searching existing data sources, gathering and maintaining the data needed, and completing and reviewing the collection of information. Send comments regarding this burden estimate or any other aspect of this collection of information, including suggestions for reducing the burden, to Department of Defense, Washington Headquarters Services, Directorate for Information Operations and Reports (0704-0188), 1215 Jefferson Davis Highway, Suite 1204, Arlington, VA 22202-4302. Respondents should be aware that notwithstanding any other provision of law, no person shall be subject to any penalty for failing to comply with a collection of information if it does not display a currently valid OMB control number.
PLEASE DO NOT RETURN YOUR FORM TO THE ABOVE ADDRESS.

1. REPORT DATE (DD-MM-YYYY) 08/30/2016		2. REPORT TYPE Software Tool		3. DATES COVERED (From - To) N/A	
4. TITLE AND SUBTITLE VIETUS - Vapor Intrusion Est. Tool for Unsat-zone Source				5a. CONTRACT NUMBER W912HQ-11-C-0023	
				5b. GRANT NUMBER	
				5c. PROGRAM ELEMENT NUMBER	
6. AUTHOR(S) Mike Truex, Pacific Northwest National Laboratory Mark Brusseau, University of Arizona Michelle Simon, US Environmental Protection Agency				5d. PROJECT NUMBER ER-201125	
				5e. TASK NUMBER	
				5f. WORK UNIT NUMBER	
7. PERFORMING ORGANIZATION NAME(S) AND ADDRESS(ES) Pacific Northwest National Laboratory - 902 Battelle Blvd, Richland, WA 99354 University of Arizona - 888 N. Euclid Room 510, Tucson AZ 85719 US EPA - 26 W Martin Luther King Drive, Cincinnati, OH 45268				8. PERFORMING ORGANIZATION REPORT NUMBER	
9. SPONSORING/MONITORING AGENCY NAME(S) AND ADDRESS(ES) ESTCP Program Office Dr. Andrea Leeson Suite 17D08 Alexandria, VA 22350				10. SPONSOR/MONITOR'S ACRONYM(S) ESTCP	
				11. SPONSOR/MONITOR'S REPORT NUMBER(S)	
12. DISTRIBUTION/AVAILABILITY STATEMENT Approved for public release; distribution is unlimited.					
13. SUPPLEMENTARY NOTES					
14. ABSTRACT The overall objective of this project is to demonstrate that the vapor-phase mass discharge test and vapor-phase tomography can effectively characterize persistent contaminant sources in the vadose zone and measure their associated mass discharge. This technology can improve evaluation of vadose-zone source impacts on groundwater and vapor intrusion. This software is a decision-support tool designed to assist users in selection and application of the technology.					
15. SUBJECT TERMS Vapor Intrusion, VI, Volatile Organic Compound, VOC, VPT, Vapor Phase Tomography					
16. SECURITY CLASSIFICATION OF:			17. LIMITATION OF ABSTRACT	18. NUMBER OF PAGES	19a. NAME OF RESPONSIBLE PERSON
a. REPORT	b. ABSTRACT	c. THIS PAGE			Mark Brusseau
U	U	U	UU	3	19b. TELEPHONE NUMBER (Include area code) 520-621-3244

Page Intentionally Left Blank

Executive Summary

Soil vapor extraction (SVE) is a prevalent remediation approach for volatile contaminants in the vadose zone. A diminishing rate of contaminant extraction over time is typically observed due to 1) diminishing contaminant mass, and/or 2) slow rates of contaminant removal from low-permeability zones. After a SVE system begins to show indications of diminishing contaminant removal rate, SVE performance needs to be evaluated to determine whether the system should be optimized, terminated, or transitioned to another technology to replace or augment SVE. For many sites, part of this evaluation will include consideration of vapor intrusion into buildings and quantification of the amount of source remediation necessary to meet vapor intrusion protection goals. This document presents a tool for estimating vapor intrusion into buildings that is a result of unsaturated (vadose) zone contaminant sources. The tool builds on, and is related to, guidance for evaluation of SVE performance relative to the impact of a vadose zone source on groundwater concentrations.

The tool described here is focused on vapor-phase diffusion from the *current* vadose zone source, and is not configured to address vapors that arise either solely from groundwater plumes (i.e., where contamination was released directly to groundwater or where a vadose zone source is not currently present) or from groundwater contamination resulting from a historically stronger vadose zone source. The spreadsheet tool uses a quantitative estimation approach that incorporates vadose zone source strength and location, vadose zone transport, and a model for estimating movement of soil-gas vapor contamination into buildings. The tool may be appropriate for a broad range of site conditions, though the user will need to assess the suitability of the underlying assumptions used in the estimation process when applying the tool. In some cases (such as significant vadose zone heterogeneities or high recharge/moisture content), site-specific modeling may be appropriate for improving estimates.

The tool described here incorporates the results of three-dimensional multiphase transport simulations predicting the vapor concentration distribution from a vadose zone source. A large number of simulations were conducted to develop a data set that can be queried based on the specific configuration of the user's site. If the user's site configuration does not exactly match one of the existing simulation configurations, interpolation is used to generate an appropriate vapor concentration estimate. With this approach, the user has access to results from transport simulations without expending the time and effort to conduct simulations themselves. This tool configuration also enables the user to rapidly conduct multiple evaluations using variations in input parameters, thereby gaining insight into the sensitivity of the results to variations in these parameters.

Page Intentionally Left Blank

Contents

Executive Summary	iii
Acknowledgments.....	v
1.0 Introduction	1
2.0 Calculational Steps	5
2.1 Compile Inputs for the Conceptual Site Model Framework	8
2.2 Interpolation from Pre-Modeled Scenario Results for Nonlinear Variables	12
2.3 Scaling for Linear Variables	14
2.4 Estimation of Vapor Intrusion.....	15
2.5 Limitations and Assumptions.....	19
3.0 Example Calculation.....	23
4.0 VIETUS User Guide.....	29
4.1 System Requirements.....	29
4.2 Installing and Starting VIETUS	29
4.3 Description of the VIETUS Workbook.....	30
4.4 Using the Software.....	33
5.0 References	35

Figures

1	Conceptual representation of the processes relevant to a constant vadose zone source at a steady-state equilibrium.....	1
2	Conceptual framework for estimating the impact of a vadose zone contaminant source on soil gas concentrations and vapor intrusion into a building.....	6
3	Categories of conceptual site models for persistent vadose zone contamination sources	7
4	Flow chart of the steps involved in the process for estimating soil gas contaminant concentration and building contaminant concentration due to vapor intrusion	8
5	Depiction of the permissible range for the gravimetric soil moisture content input parameter, the corresponding values of residual saturation, and how the ranges are reconciled at the lower and upper limits	10
6	Example of the spatial interpolation from numerical grid cell centers to the location of interest within the bounds of those cell centers	24
7	View of the primary data on the “HLC” worksheet of the VIETUS workbook	30
8	Groupings of worksheet cells into blocks for input parameters, intermediate calculations, and results.....	31
9	View of the “VIETUS” worksheet, showing details of the input parameters, intermediate calculations, results, and reference information.....	32

Tables

1	Parameters defining source and transport site characteristics used in the estimation of soil gas concentration	9
2	Input parameters defining vapor intrusion characteristics	11
3	Categorization of pairs of <i>VZT</i> and <i>STR</i> values to assist in data organization.....	13
4	Tabulated correlation coefficients for calculating vapor pressure and solubility of contaminants of interest.....	14
5	Typical ranges of parameter values for residential buildings taken from EPA guidance.....	16
6	Tabulated correlation coefficients for calculating the gas diffusion coefficient for contaminants of interest.....	18
7	User input for the scenario variants applied in the example calculations for estimation of the soil gas concentrations and vapor intrusion	23
8	Parameter values for the example cases that are used in the second phase of interpolation.....	24
9	Sequential interpolation to determine C_{gu} for Cases A and B of the example	25

1.0 Introduction

Soil vapor extraction (SVE) is a prevalent remediation approach for volatile contamination in the vadose (unsaturated) zone of the subsurface. A diminishing rate of contaminant extraction over time is typically observed due to 1) diminishing contaminant mass in the vadose zone source, and/or 2) slow rates of contaminant removal from low-permeability zones. After a SVE system begins to show indications of diminishing contaminant removal rate, SVE performance needs to be evaluated to determine whether the system should be optimized, terminated, or transitioned to another technology to replace or augment SVE. For many sites, part of this evaluation will include consideration of vapor intrusion into buildings and quantification of the amount of source remediation necessary to meet vapor intrusion protection goals.

This document presents an approach and a tool for estimating vapor intrusion resulting from vadose zone contaminant sources, as depicted in Figure 1. The tool may be appropriate for readily obtaining estimates for a broad range of site conditions. However, the user needs to consider the underlying assumptions and limitations (see Section 2.5) of the estimation process when applying the tool. *The tool described here is focused on vapor-phase diffusion from the **current** vadose zone source, and is not configured to address vapors that arise either solely from groundwater plumes (i.e., where contamination was released directly to groundwater or where a vadose zone source is not currently present) or from groundwater contamination resulting from a historically stronger vadose zone source.* Further, the nature of the underlying generalized conceptual site model necessitates various assumptions and bounds for site configuration. Thus, a site-specific model may be useful for detailed analysis of some sites.

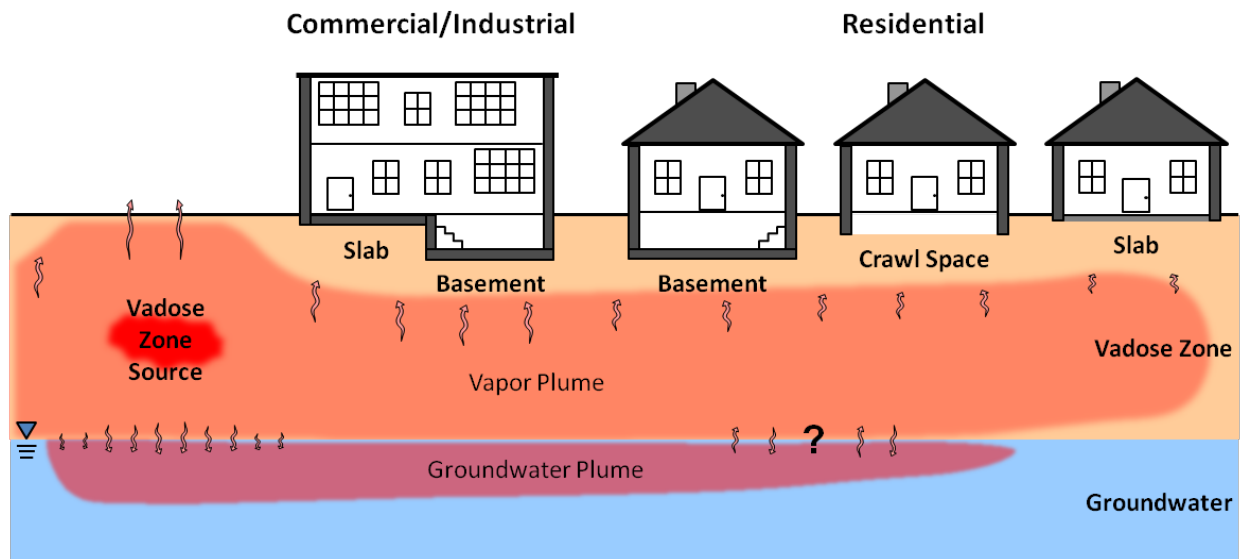


Figure 1. Conceptual representation of the processes relevant to a constant vadose zone source at a steady-state equilibrium. Contaminant vapor diffuses out from the source and may travel within the vadose zone or leave the vadose zone 1) at the ground surface, 2) via vapor intrusion into buildings, or 3) by mass transfer into groundwater (near the source or at distance from the source). Groundwater contaminated by the vadose zone source may travel downgradient by advection/dispersion, and contamination could transfer back into the vadose zone (depending on the chemical properties and concentration gradients).

When vapor-phase transport is the major component of the overall contaminant fate and transport from a vadose zone source, the contaminant concentration expected at a given subsurface location is controlled by a limited set of parameters describing source and subsurface characteristics. Thus, it is possible to pre-model contaminant transport for a range of conditions and to estimate the results for a specific waste site based on these pre-modeled scenarios. This approach has previously been applied in the Soil Vapor Extraction Endstate Tool (SVEET) software [Truex et al., 2013; Oostrom et al., 2014]. The tool described herein incorporates the results of three-dimensional multiphase transport simulations (described in detail by Truex et al. [2013] and Oostrom et al. [2014]) predicting the steady-state vapor concentration distribution resulting from a vadose zone source. A large number of simulations were conducted to develop a data set that can be queried based on the specific configuration of the user's site. If the user's site configuration does not exactly match one of the existing simulation configurations, interpolation and scaling (e.g., to account for differences in Henry's Law constants) are used to generate an appropriate vapor concentration estimate. With this approach, the user has access to results from transport simulations without expending the time and effort to configure a model and conduct simulations themselves. This pre-modeled scenario approach allows the user to rapidly conduct multiple evaluations using variations in input parameters, thereby gaining insight into the sensitivity of the results to variations in these parameters.

The simulations conducted for the pre-modeled scenarios predict soil gas concentrations for a range of subsurface conditions where transport from the vadose zone source occurs predominantly by vapor-phase diffusion. That is, the subsurface vadose zone is relatively dry and there is low recharge (infiltration) through the vadose zone. The pre-modeled scenario simulations included three-dimensional contaminant movement from the vadose zone source (both by diffusion and along with recharge). Vapor-phase contamination could exit the vadose zone at the ground surface or could partition into the groundwater. Contamination in the groundwater, from vapor-phase partitioning or recharge influx, migrated downgradient with the groundwater, but without any adsorption or bio/geochemical reactions. Back-transfer of contamination from groundwater to the vadose zone at downgradient locations could occur, depending on the concentration gradient.

The pre-modeled simulations represent neither historical groundwater contamination nor groundwater contamination in the absence of the current vadose zone source. That is, the simulations start with clean groundwater and only represent groundwater contamination resulting from the defined vadose zone source. The intent of this approach was to allow evaluation of whether the residual source remaining after termination of SVE is predicted to result in a vapor intrusion issue (assuming sufficient time to produce a steady-state vapor plume). Such evaluation would support decisions regarding optimization, termination, or transition of the SVE remedy. However, the evaluation approach described here does not provide insight into vapor intrusion resulting from pre-existing groundwater contamination (i.e., that does not arise from the current defined vadose zone source).

The estimated soil gas contaminant concentration obtained from the pre-modeled scenarios for a building location of interest is combined with an analytical solution adapted from Johnson and Ettinger [1991] to estimate the vapor intrusion into the building. This is a different approach, in that the soil-gas contaminant concentration below the building is determined independently and then the entry rate of contaminant into the building is equated to the rate of contaminant removal via ventilation. This allows calculation of the indoor air concentration. The Johnson and Ettinger [1991] model included equations for diffusive transport of contaminant in vadose zone soil gas from a source (nominally groundwater below the building) and calculated an attenuation factor representing the ratio of indoor air concentration

to the source concentration. With the independent calculation of concentration in the soil gas below the building applied in the approach described here, there is not a linkage between diffusive flux and rate of vapor intrusion. That is, the advective flow into the building (driven by the building under-pressure and air-exchange with the outside) does not influence the contaminant transport through the vadose zone. As noted by the EPA [2004], the zone of influence for advective contaminant flow is expected to be limited to a region adjacent to the building foundation.

The overall vapor intrusion estimation approach consists of four steps: 1) defining site-specific inputs, 2) interpolating between pre-modeled scenario results based on parameters that have nonlinear impacts on the soil gas contaminant concentration, 3) scaling the interpolated result based on parameters that have linear impacts on the soil gas contaminant concentration, and 4) estimating the contaminant concentration in a building due to vapor intrusion. The first three steps result in an estimate of the steady-state soil-gas contaminant concentration at a depth and lateral distance representing the location just beneath the building of interest. The soil gas concentration is then used as part of the input to the adapted Johnson and Ettinger [1991] vapor intrusion calculations. For user convenience, the calculational steps are incorporated into the Vapor Intrusion Estimation Tool for an Unsaturated-zone Source (VIETUS) software, which is a spreadsheet-based (Microsoft Excel) tool.

This report describes the calculational steps and basis for the approach, provides an example to illustrate the calculations, and provides a guide for using the VIETUS spreadsheet tool.

2.0 Calculational Steps

The approach for estimating a soil-gas contaminant concentration in the vadose zone and the corresponding gas concentration in a building due to vapor intrusion is based on a generalized conceptual site model and, as mentioned previously, is comprised of several calculational steps.

The generalized conceptual model describes a site with a vadose zone source that remains constant over time, resulting in a steady-state distribution of vapor-phase contamination in the vadose zone. Vapor-phase transport by diffusion from the source zone is taken as the dominant transport mechanism. The nature of the porous media means that the effective gas diffusion in the subsurface is less than that of diffusion in air (because of the pore structure of the soil and a portion of the pore space being filled by moisture). Thus, transport predominantly by diffusion implies low moisture content and low recharge conditions. Because the approach focuses on steady-state conditions, moderate heterogeneities have limited impact on the vapor-phase concentration distribution [Truex et al., 2013] and a homogenous subsurface approximation can be used for the conceptual model. However, if a site has significant heterogeneities, site-specific modeling may be appropriate for improving estimates. Higher recharge and wetter vadose zone environments lead to additional complexity in contaminant transport, especially with respect to interaction with the groundwater. Such conditions are outside the range of the simulations conducted to support the calculational approach and would also require site-specific modeling.

The generalized conceptual model includes contaminant partitioning into and out of the groundwater beneath the source area because this is an important boundary condition for vapor-phase transport. Because the approach is intended to supply information to support a decision about SVE disposition, the calculations focus solely on the contribution to vapor intrusion from the current vadose zone source. Specifically, the only groundwater contamination contributions included are those directly resulting from the current vadose zone source conditions.

The user should consider that the generalized conceptual model and associated calculation approach include simplifications of actual site conditions. The approach, however, enables a user to relate contaminant mass discharge (or source concentration) from a vadose zone source to a predicted steady-state vapor-phase concentration at a specified location for a depth underneath the building of interest. The soil gas concentration can then be used in estimating potential vapor intrusion. The user should consider estimate uncertainties in light of the site conditions to interpret whether the estimated vapor intrusion concentrations are acceptable or not.

The generalized conceptual site model, depicted in Figure 2, provides a method for specifying the key input parameters in a framework that can be adapted for a variety of sites. The generalized conceptual site model represents the source area as a zone with specified dimensions (i.e., areal footprint, thickness, and depth within the vadose zone) and contaminant “strength.” The subsurface is assumed to be a uniform, homogeneous material with specified characteristics (e.g., temperature, moisture content) and fixed values of porosity (0.3), bulk density (1.855 g/mL), and recharge (0.4 cm/yr). Groundwater beneath the vadose zone flows at a specified rate (Darcy velocity), with the orientation of the conceptual model such that groundwater flow is parallel to the x-axis (left to right in the figure). The model is configured to maximize partitioning across the water table, thus assumes a minimal capillary fringe. Contaminants can partition into the groundwater, move along with the groundwater flow, and, if conditions are appropriate, partition back into the vadose zone. A single building is assumed to be located at a specified lateral

distance from the center of the source area, not necessarily on the axis of the model. Characteristics pertaining to vapor intrusion through the foundation (e.g., foundation thickness, ventilation rate, area of cracks, etc.) must be defined for the building.

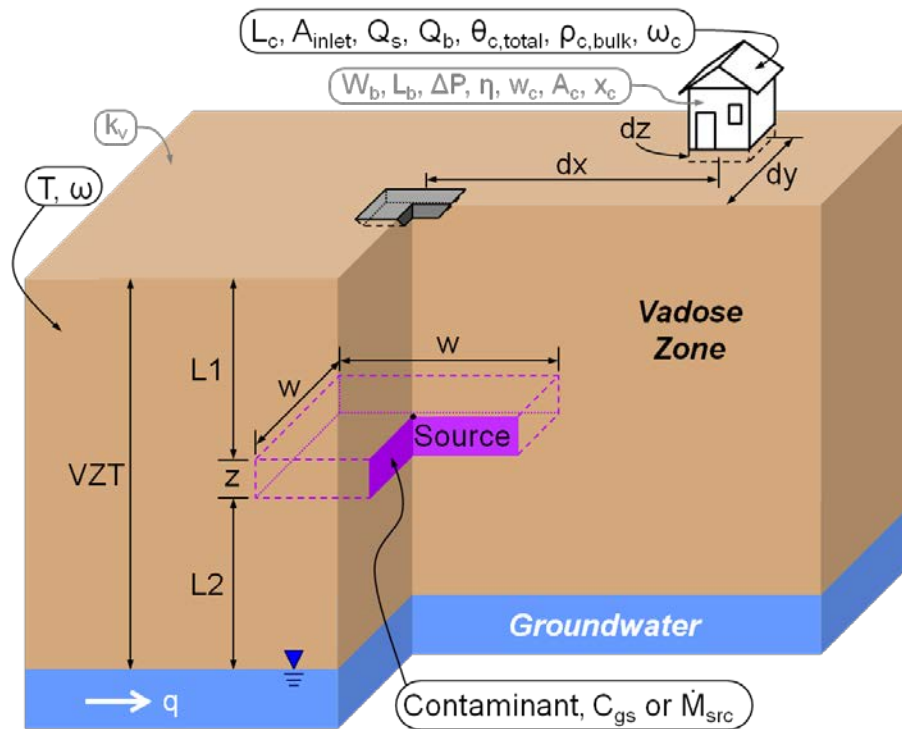


Figure 2. Conceptual framework for estimating the impact of a vadose zone contaminant source on soil gas concentrations and vapor intrusion into a building; Tables 1 and 2 describe the variables.

If the framework of the generalized conceptual site model, including the valid ranges of parameter values (Section 2.1) and the simplifying assumptions (Section 2.5), is not appropriate for a given site, then an alternative calculational approach would be required. For example, sites with significant heterogeneity/layering, widely dispersed contaminant sources, significant contaminant sources in the groundwater, significantly different moisture content, or significantly different recharge conditions may need to use a site-specific numerical model (e.g., STOMP [White and Oostrom, 2006]) for an improved estimate of the soil gas concentration distribution.

While each site is unique, there are three general categories of vadose zone contaminant sources, as depicted in Figure 3. These categories reflect common types of subsurface heterogeneities and are based on the premise that vadose zone contaminant sources are persistent because they reside within lower permeability zones or areas that are poorly swept by a SVE system (e.g., high moisture zones). For many sites, persistent vadose zone contaminant sources would be expected to exist within a localized portion of the vadose zone as a remnant of contaminant transport pathways that occurred during the waste disposal period. For sites with widely dispersed remaining sources and unique subsurface features, a site-specific analysis may be more appropriate. However, for sites where the remaining sources are more localized, the generalized conceptual model may be representative of the source area(s).

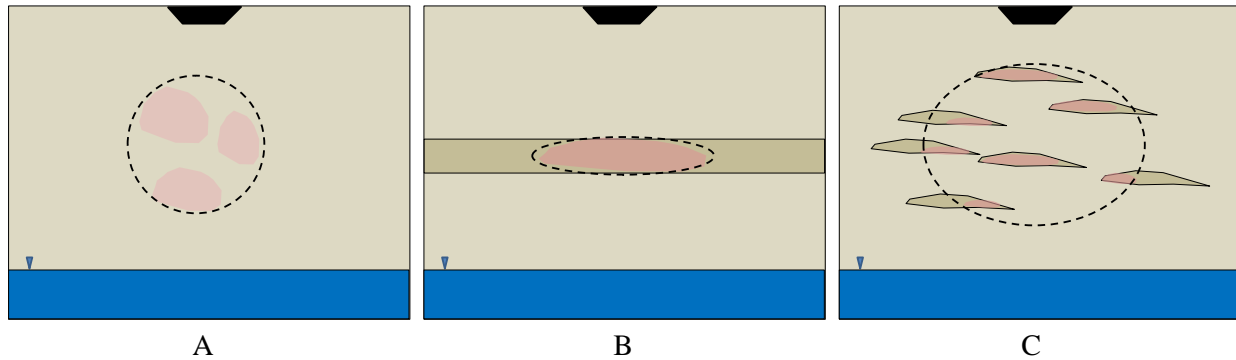


Figure 3. Categories of conceptual site models for persistent vadose zone contamination sources. A) homogenous subsurface with residual source; B) simple layered subsurface with source accumulation in low permeability material; and C) multiple layers or lenses in the subsurface with source accumulation in low permeability material. Red = contamination source; blue = groundwater; tan = high permeability; brown = low permeability; black = waste disposal site. The dashed lines show zones where, over time, vapor concentrations will nominally equilibrate to a composite source concentration as a result of diffusion from the specific source zones.

While the nature of the subsurface is significantly different for the three conceptual model categories shown in Figure 3, the vadose zone source may be approximated in each case as a single zone of specified dimension and concentration/source strength (Figure 2). This generalized source is most apparent for Figure 3(B), where remaining contaminants reside primarily in a distinct low-permeability layer. However, in both Figure 3(A) and 3(C), the contamination resides within a defined volume of the vadose zone and a composite concentration can be assigned. That is, for the scenarios shown in Figures 3(A) and 3(C), vapors may emanate from smaller distinct portions of the composite source zone, but in the long term, vapor concentrations will equilibrate in some zone between and around these distinct sources (as represented by the dashed outlines on the figures). The result is an effective composite source zone that acts as the source concentration that drives diffusion out into the vadose zone and eventually to the surface or the groundwater. Aqueous recharge moving through this zone will become contaminated. However, the concentration of the pore water at the water table will be in equilibrium with the vapor concentration at that location. Thus, for sites with relatively low recharge rates, the composite vapor concentration will also be a primary factor in the long-term aqueous phase contaminant discharge to the groundwater.

A site may also have heterogeneities outside of the source zone in the form of distinct layers or lenses with lower-permeability and/or higher moisture content than the bulk vadose zone materials. However, in Truex et al. (2013; in their Appendix E) conducted simulations to evaluate long-term vapor transport in the presence of lower permeability layers with moderately higher moisture content than the bulk vadose zone. Although the effective diffusion coefficient is lower for the increased moisture content in the lower permeability layers, the subsurface vapor-phase contaminant concentration distribution was only minimally affected by such layers when looking at long-term steady-state conditions. Thus, for moderate subsurface heterogeneities, the use of the homogenous approximation in the generalized conceptual model may be appropriate. Users will need to consider the level of heterogeneity at their site and assess the appropriateness of the generalized conceptual model, using site-specific modeling for the vapor intrusion assessment if the generalized conceptual model is insufficient for their site.

The four steps of the calculational approach implemented in the VIETUS software are shown in Figure 4, and are discussed in detail in the sections below. Section 3.0 walks through an example calculation to further illustrate these steps.

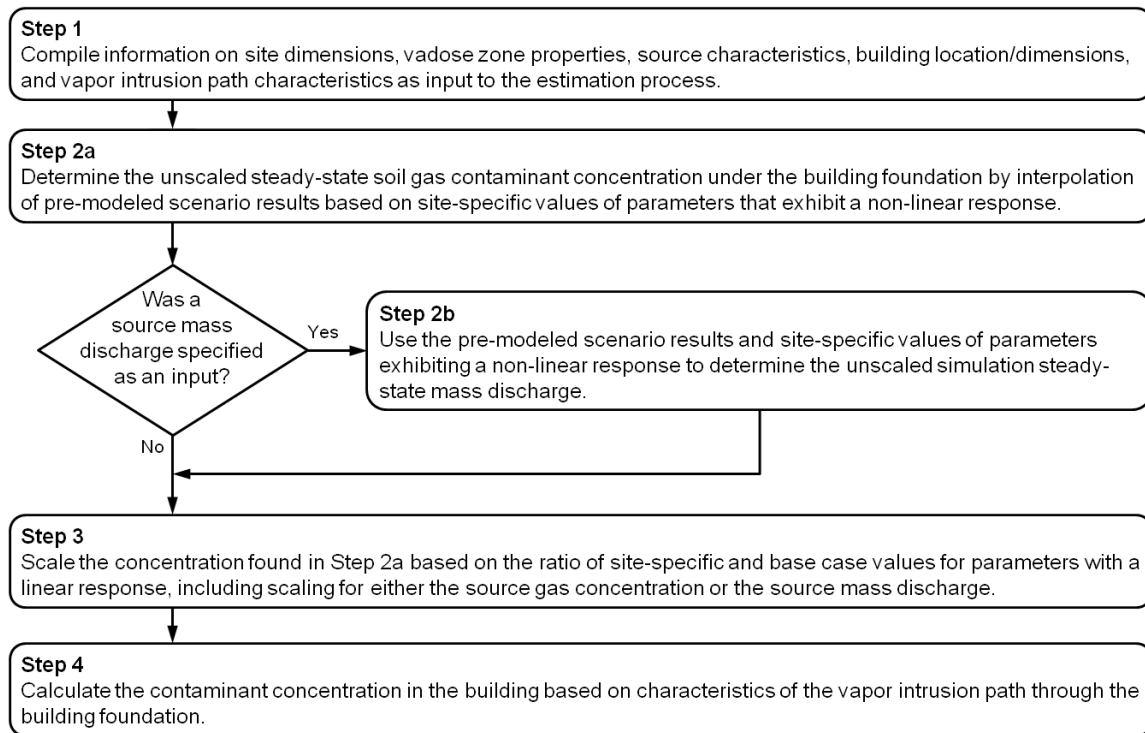


Figure 4. Flow chart of the steps involved in the process for estimating soil gas contaminant concentration and building contaminant concentration due to vapor intrusion; Sections 2.1 through 0 correspond to these four steps.

2.1 Compile Inputs for the Conceptual Site Model Framework

The framework of the generalized conceptual site model (Figure 2) requires a set of inputs to describe each scenario of interest. The input parameters listed in Table 1 describe the source- and transport-related characteristics that must be compiled (with vapor intrusion parameters being discussed later in this section). These inputs are used to calculate several intermediate parameters. The inputs (or the appropriate intermediate parameter) define the interpolation between pre-modeled scenarios (for parameters exhibiting a nonlinear response in the results) and the linear scaling from the base case scenario to the site-specific scenario. To avoid extrapolation outside of the pre-modeled scenarios, the input parameters are restricted to be within the permissible ranges noted in Table 1. Ranges have also been defined for parameters that exhibit a linear or inverse linear relationship to contaminant concentrations (including the “source strength” parameters). The source strength input parameters (C_{gs} and \dot{M}_{src}) have upper bounds nominally based on levels where density-driven advection would not affect contaminant migration. The range for Henry’s Law constant is constrained by the choice of the contaminant and the permissible range for the subsurface temperature.

Table 1. Parameters defining source and transport site characteristics used in the estimation of soil gas concentration (*shaded rows are calculated parameters; rows without shading are user inputs*)

Parameter Name	Units	Variable	Permissible Range	Key Values ^a
<i>INPUT PARAMETERS USED TO CALCULATE OTHER PARAMETERS</i>				
Contaminant	—	—	Carbon Tetrachloride Chloroform Dichloromethane Chloromethane Tetrachloroethene Trichloroethene Dichloroethene isomers Vinyl Chloride 1,1,1,2-Tetrachloroethane 1,1,2,2-Tetrachloroethane 1,1,1-Trichloroethane 1,1,2-Trichloroethane 1,1-Dichloroethane 1,2-Dichloroethane Chloroethane	Carbon Tetrachloride
Average subsurface temperature	°C	<i>T</i>	10 – 30	20
Depth to the top of the source zone	m	<i>L1</i>	0.5 – 49	—
Vertical thickness of the source zone	m	<i>z</i>	1 – 30	—
Width for plan view extent of source (source is assumed square, thus width = length)	m	<i>w</i>	10 – 50	—
<i>PARAMETERS HAVING A NONLINEAR IMPACT ON CONCENTRATIONS</i>				
Average gravimetric moisture content in vadose zone ^b (mass of water per mass of dry porous medium)	wt%	ω	1 – 9	1, 5, 9
Vadose zone thickness	m	<i>VZT</i>	10 – 60	10, 30, 60
Source thickness ratio (fraction of vadose zone thickness that is source material) ($STR = z / VZT$)	—	<i>STR</i>	0.1 – 0.5	0.1, 0.25, 0.5
Relative vertical source position in the vadose zone (i.e., near surface, aquifer or middle) ($RSP = L1 / L2 = L1 / [VZT - L1 - z]$)	—	<i>RSP</i>	0.1 – 10	0.1, 1, 10
Source area as a plan-view areal extent ($SA = w^2$)	m ²	<i>SA</i>	100 – 2500	100, 400, 900, 2500
Groundwater Darcy velocity (<i>q</i> is input directly, but can be calculated from $q = K_h \cdot i$, with K_h = horizontal hydraulic conductivity, <i>i</i> = hydraulic gradient)	m/d	<i>q</i>	0.005 – 0.3	0.005, 0.03, 0.3
<i>PARAMETERS HAVING A LINEAR (OR INVERSE LINEAR) RELATIONSHIP WITH SOIL GAS CONCENTRATION</i>				
Henry's Law constant ^c	—	<i>H</i>	contaminant-specific	0.89
Gas-phase contaminant concentration in the source ^d	ppmv	C_{gs}	0.1 – 2000	159
Mass discharge of vapor-phase contamination from the source ^d	g/d	\dot{M}_{src}	0.1 – 5000	varies

^a The key values indicate either the values used in the pre-modeled scenario simulations (for parameters having nonlinear relationship) or the “base case” scenario values (for parameters having a linear/inverse linear or source strength relationship). Base case recharge was 0.4 cm/yr, but recharge is not a site-specific input. The pre-modeled scenario simulations are discussed in more detail in Section 2.2.

^b The pre-modeled scenario simulations (Section 2.2) actually use the residual water saturation (S_r), which is calculated from moisture content as: $S_r = (\omega \cdot \rho_{bulk}) / (100 \cdot \theta_{total} \cdot \rho_{water})$, where ρ_{bulk} is the dry bulk density of the porous media (1.855 g/mL), θ_{total} is the total porosity (0.3), and ρ_{water} is the (temperature-dependent) density of water. The range for S_r was 0.05 to 0.55 in the simulations, so ω is constrained accordingly, as discussed in the text in below.

^c The dimensionless Henry's Law Constant is based on the site-specific subsurface temperature and contaminant-specific, temperature-dependant property correlations for vapor pressure [Yaws et al., 2009] and solubility [Mackay et al., 2006; Yaws, 2003].

^d The user may provide either C_{gs} or MD_s , but not both. The mass discharge “key values” are interpolated from the pre-modeled scenario simulation results.

Note that, while gravimetric soil moisture content (ω) is requested as an input parameter (Table 1) for user convenience, residual saturation (S_r) is the actual parameter specified in the pre-modeled scenario simulations (Section 2.2). S_r is calculated from ω as discussed in the footnotes to Table 1. The key values for S_r were 0.05, 0.3, and 0.55, which correspond to moisture content values of 0.8071721, 4.843, and 8.87889, respectively, for a subsurface temperature of 20 °C. To keep the information concise, the permissible moisture content range is specified in Table 1 and the VIETUS software as 1 to 9 wt%. Values at or above 8.87889 wt% are treated as S_r values of 0.55. If the “Allow ω down to $S_r = 0.05$?” option (discussed in Section 4.4) is set to TRUE, then ω values down to 0.8071721 wt% (at 20 °C) are allowed. Otherwise, ω values below 1 wt% result in an incomplete calculation (because the value is outside the permissible range). The specific weight percent numbers mentioned above vary slightly as a function of temperature because the density of water is a function of temperature. Figure 5 depicts the permissible range for ω and the corresponding values of S_r . Note that the numbers discussed above include sufficient significant digits to obtain precision in the appropriate conversion calculations.

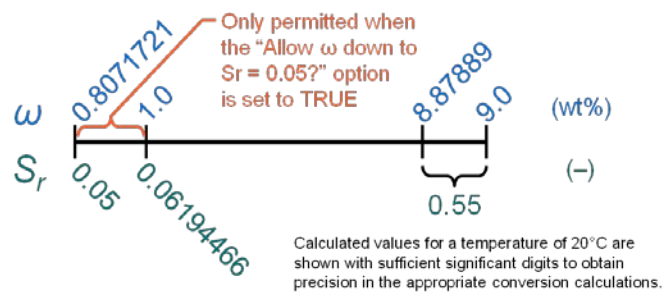


Figure 5. Depiction of the permissible range for the gravimetric soil moisture content input parameter (ω), the corresponding values of residual saturation (S_r), and how the ranges are reconciled at the lower and upper limits

Appendix A of Truex et al. [2013] discusses approaches for determining or estimating certain information about the source area, including the lateral extent, location within the vadose zone, and “source strength.” The source strength calculational input may be represented as either a constant vapor-phase contaminant concentration (C_{gs}) or mass discharge of contaminant (\dot{M}_{src}), but not both.

Input parameters for calculating vapor intrusion (migration of contaminant from soil gas into a building) are based on the Johnson and Ettinger [1991] model, with numerical simulation results used for the transport component. Unlike the Johnson and Ettinger [1991] model, the VIETUS calculational approach estimates a vapor-phase contaminant concentration in the subsurface below the building, based on numerical simulations for three-dimensional, multi-phase transport from the defined vadose zone source area. The vadose zone source strength is held constant and a steady-state vapor-phase contaminant distribution is determined in the numerical simulations. This approach thus ties the independently calculated subsurface vapor-phase contaminant concentration to the contaminant entry into a building, which is determined from the Johnson and Ettinger [1991] model. This coupling of soil-gas concentration distribution from pre-modeled scenarios to the contaminant influx to the building in the VIETUS software allows the user to quickly set up and assess multiple building scenarios. However, the results can differ from the Johnson and Ettinger [1991] model. One difference is that the Johnson and Ettinger [1991] model allows the vapor-phase concentration below the building to vary to achieve equilibrium between the diffusive flux through the soil and the advective/diffusive flux into the building. The pre-modeled simulations do not include advective movement of soil gas, either by barometric pumping or driven by building under-pressure. However, EPA [2004] describes the influence of

convection resulting from inflow to a building as only affecting the zone immediately adjacent to the foundation. Still, VIETUS results may not fully account for relevant advection when the building is laterally situated near the source area.

The vapor intrusion parameters required for use of the VIETUS tool describe the foundation, gas flow pathways through the foundation, and the building. Table 2 lists the input parameters relevant to vapor intrusion calculations in three categories. The first group includes key parameters required for the calculations, the second group are key parameters that can either be directly specified or can be calculated from secondary parameters (based on certain assumptions), and the third group consists of those secondary parameters.

Table 2. Input parameters defining vapor intrusion characteristics

Parameter Name	Units	Variable	Permissible Range
<i>KEY VAPOR INTRUSION PARAMETERS (directly specified)</i>			
Longitudinal distance to the building (from the source center to the center of the building)	m	dx	-950 – 950 ^a
Longitudinal distance to the building (from the source center to the center of the building)	m	dy	0 – 470
Depth of basement/foundation	m	dz	0.5, 1, 1.5, 2, 2.5, 3, 3.5, or 4
Foundation/wall thickness	m	L_c	0.1 – 0.61 ^b
Building ventilation rate	m ³ /d	Q_b	1,200 – 10,000 ^c
<i>KEY VAPOR INTRUSION PARAMETERS (calculated from secondary parameters or directly specified)</i>			
Gas flow rate into the building from the soil	m ³ /d	Q_s	$0 < Q_s \leq (x_c/40) \cdot 15^{b,c}$
Area of cracks or foundation	m ²	A_{inlet}	varies ^{b,d}
Total porosity within the cracks/foundation	—	$\theta_{c, total}$	0.01 – 0.9
Gas-filled porosity within the cracks/foundation	—	$\theta_{c, g}$	$\leq \theta_{c, total}$
<i>SECONDARY VAPOR INTRUSION PARAMETERS</i>			
Vapor intrusion path type	—	—	Cracks, Porous foundation
Total area of cracks	m ²	A_c	$< 4 \cdot x_c \cdot dz$
Building under-pressure	Pa	ΔP	0 – 20
Soil gas permeability	m ²	k_v	1E-10 – 1E-16
Crack ratio (area of cracks / area of foundation)	—	η	0.0001 – 0.002
Crack width	m	w_c	0.0005 – 0.01
Building width	m	W_b	> 2 and $W_b \cdot L_b < 900$
Building length	m	L_b	> 2 and $W_b \cdot L_b < 900$
Cumulative lateral crack length	m	x_c	$> A_c / (4 \cdot dz)$

^a Negative distances are located upgradient (with respect to groundwater flow direction) from the source area.

^b The combination of the foundation/wall thickness, L_c , the crack/foundation area, A_{inlet} , the gas diffusion coefficient for the cracks/foundation, D_c , and the Q_s value must not cause the exponential function to result in an error in the following expression: $\exp[(L_c \cdot Q_s)/(A_{inlet} \cdot D_c)]$. If the site configuration causes an error in the $\exp()$ term, refer to equation 22 of Johnson & Ettinger [1991].

^c The upper limit shown for Q_b is a soft limit, with a hard limit applied at a value of 80,000 m³/d. The upper limit shown for Q_s is a soft limit, with a hard limit applied at a value of $0.06 \cdot Q_b$ (which is twice the observed top end sub-slab to indoor air attenuation factor [EPA, 2012]).

^d Clearly, the area of cracks cannot exceed the area of the subsurface foundations. Typically, the area of cracks is less than 0.2% of the area of the subsurface foundations.

The key parameters for vapor intrusion calculations define the location of the building with respect to the vadose zone contamination source and gas flow into the building (whether through a slab foundation or into a sub-grade basement). The lateral location of the building and depth of the foundation are used to determine the soil gas concentration underneath the building (based on numerical transport simulation results). Whether the lateral location represents the center of the building footprint or another location of interest, a single soil gas value is used to calculate vapor intrusion.

Johnson and Ettinger [1991] describe several scenarios and apply some simplifying assumptions to arrive at estimates of migration of contaminant through a foundation. The first scenario they considered involves cracks in the foundation, through which gas (and contaminant) flows because of building under-pressure. In the crack scenario, the area of the cracks is specified and cracks are assumed to be filled with porous media having the same porosity, bulk density, and moisture content as the soil underneath the foundations. In addition, Johnson and Ettinger [1991] estimate the volumetric flow rate of soil gas into the building based on an idealized model of cracks being located at floor/wall seams. The other scenario they considered is vapor intrusion through a porous foundation, in which case soil gas flows through foundation pores across the entire sub-grade portion of the foundation. These scenarios and assumptions provide context for what input parameters are needed for the calculations to estimate vapor intrusion. Section 0 discusses the vapor intrusion parameters in more detail.

Because of the uncertainty associated with input parameters, users are encouraged to conduct the estimation process using a sensitivity analysis approach. In such an approach, multiple estimates are made using appropriate ranges for input parameter values and the effect of these variations on the estimated soil-gas contaminant concentration can be assessed. The spreadsheet tool (Section 4.0) allows multiple input scenarios to be evaluated as a group.

2.2 Interpolation from Pre-Modeled Scenario Results for Nonlinear Variables

A total of 972 pre-modeled scenarios were simulated with the Subsurface Transport Over Multiple Phases (STOMP) code [White and Oostrom, 2006] to assess the impact on results when parameters that exhibit a nonlinear response are varied. Simulations were run for each scenario to obtain steady-state concentration distributions in the gas and aqueous phases throughout the computational domain, assuming a constant-strength vadose zone source. These pre-modeled scenarios all used “base case” values for parameters exhibiting a linear response, including values of 0.4 cm/yr of recharge, a carbon tetrachloride source at a soil-gas concentration of 1 mg/L_{gas} (159 ppmv), and a Henry’s Law constant of 0.89. The base case also used a porosity of 0.3, a dry bulk density of 1855 kg/m³, a gas diffusion coefficient of 0.0845 cm²/s, and a liquid diffusion coefficient of 8.62E-6 cm²/s. Table 1 lists the key values used in the simulations for each of the parameters with a nonlinear relationship to contaminant concentrations. It is the combinations of these key parameter values that comprise the suite of 972 pre-modeled scenarios. Key parameter values were selected to allow linear interpolation between simulation results (i.e., for bounding key values) to provide a reasonable estimate of the soil-gas concentration at any given parameter value (within the bounds of the key values). Note that the pre-modeled simulations used for VIETUS are the same set of simulations as used for the SVEET software [Truex et al., 2013].

The interpolation step in the estimation of the soil-gas contaminant concentration is based on a sequence of data lookups and linear interpolations to find the unscaled gas concentration (C_{gu}) for the site-specific

input parameters. Interpolation is needed for parameters and when site-specific parameter input values differ from key values. Interpolated values are calculated using Equation 1, where P denotes the parameter value, C is the simulation concentration, and the subscripts *upper* and *lower* represent the known values corresponding to key values above and below the interpolation point of interest (*interp*).

$$C_{interp} = \left[\frac{P_{interp} - P_{lower}}{P_{upper} - P_{lower}} \right] \cdot (C_{upper} - C_{lower}) + C_{lower} \quad (1)$$

Spatial interpolation is generally required between soil-gas concentration results at grid-cell centers in the numerical model to obtain a concentration result at the site-specific vertical and lateral location. Soil gas concentrations at the center of grid cells were tabulated for each pre-modeled scenario to allow spatial interpolation across the model domain down to a depth of four meters below ground surface. Thus, interpolation can be performed, as needed, to determine the soil gas concentration at the vertical location, dz , and lateral location (specified by dx and dy) of interest.

A set of 2^6 pre-modeled scenarios provide simulation soil-gas concentration values (C_{sim}) for a given location (at dx , dy , and dz) that can be used for parameter-based interpolation related to the six parameters that exhibit a nonlinear contaminant concentration response (RSP , q , SA , VZT , STR , and S_r ; described in Table 1). These 64 values represent 32 pairs of concentrations for scenarios with parameter key values that are both above and below (or equal to) the site-specific parameter value. Interpolation between parameter key values proceeds, first for RSP , then q , and so on for SA , VZT , STR , and S_r , to arrive at a value for C_{gu} . Note that S_r is the water saturation value converted from the ω moisture content value (as discussed in the footnotes to Table 1).

If the source strength input parameter was provided as a \dot{M}_{src} value (i.e., not a C_{gs} value), then a second sequence of lookups/interpolations (in the same order of RSP , q , SA , VZT , STR , and S_r) is performed to determine the simulated contaminant mass discharge (\dot{M}_{sim}) corresponding to the input site parameters. This \dot{M}_{sim} value is needed as a linear scaling factor. The process for obtaining the interpolated \dot{M}_{sim} mass discharge value is the same as for C_{gu} , except that spatial interpolation does not apply.

For convenience, the key VZT and STR parameter values are paired and assigned a Source Assessment Category designation, as shown in Table 3. It is infeasible to assemble the C_{sim} data for soil gas concentrations into discreet tables organized by these categories because the soil gas data is comprised of multiple full layers of data and is about 75 MB when stored as an uncompressed, plain text file. However, the category terminology is useful nomenclature, consistent with SVEET [Truex et al., 2013].

Table 3. Categorization of pairs of VZT and STR values to assist in data organization

	VZT (m)		
STR (-)	10	30	60
0.1	Category 1	Category 2	Category 3
0.25	Category 4	Category 5	Category 6
0.5	Category 7	Category 8	Category 9

2.3 Scaling for Linear Variables

The third step in the estimation procedure is to scale the C_{gu} value obtained from the interpolation step to account for the parameters where the soil gas contaminant concentration varies linearly or inverse linearly with the parameter value. The base case (key) values discussed above and listed in Table 1 form the basis for the scaling.

The Henry's Law constant for the site conditions (contaminant and temperature) is required as part of the scaling process. In Table 1 it was noted that the Henry's Law constant can be calculated based on the site-specific subsurface temperature and contaminant-specific, temperature-dependent property correlations. The Henry's Law constant and its temperature dependence have been examined in a wide range of literature for contaminants of environmental interest [e.g., Staudinger and Roberts, 2001; Warneck, 2007; Chen et al., 2012]. Brennan et al. [1998] suggest calculating the Henry's Law constant as the ratio of the vapor pressure to the water solubility as the preferred approach for dilute contaminant concentrations (< 0.02 mol fraction). Thus, a temperature-dependent Henry's Law constant can be found using temperature-dependent vapor pressure and water solubility values. However, the accuracy of this approach depends on the accuracy of the vapor pressure and water solubility information.

The temperature-dependent vapor pressure correlation selected for use in this work is the Antoine correlation given in Equation 2 where T is temperature in °C, P_{vap} is the vapor pressure in mm Hg, and A , B , and C are contaminant-specific correlation coefficients [Yaws et al., 2009], listed in Table 4.

$$\text{Log}_{10}(P_{vap}) = A - \frac{B}{T + C} \quad T \text{ is in } ^\circ\text{C} \text{ and } P_{vap} \text{ is in mm Hg} \quad (2)$$

Table 4. Tabulated correlation coefficients for calculating vapor pressure and solubility of contaminants of interest, taken from Yaws et al. [2009], Mackay et al. [2006], and Yaws [2003]

Contaminant Abbrev.	Contaminant	Molecular Weight (g/mol)	Correl. Coef. for Calculating Vapor Pressure			Correlation Coefficients for Calculating Solubility					
			A	B	C	A	B	C	D	E	F
CT	Carbon Tetrachloride	153.823	7.01144	1278.54	232.888	9.7842 E-2	-1.4942 E-3	3.5854 E-5	2.2775 E-7	0	0
CF	Chloroform	119.378	7.11148	1232.79	230.213	9.9500 E-1	-1.0531 E-2	7.9819 E-5	6.6431 E-7	0	0
DCM	Dichloromethane	84.933	7.11464	1152.41	232.442	1.9610	-4.4883 E-2	8.6617 E-4	4.9463 E-6	0	0
CM	Chloromethane	50.488	6.99771	870.17	235.586	1.4019	-6.3562 E-2	1.7198 E-3	-2.8262 E-5	2.5268 E-7	-9.3470 E-10
PCE	Tetrachloroethene	165.833	7.06892	1458.45	226.986	2.6479 E-1	-1.5487 E-3	2.4477 E-6	0	0	0
TCE	Trichloroethene	131.388	6.87981	1157.83	202.58	1.4049	-8.2223 E-3	1.3218 E-5	0	0	0
1,1-DCE	1,1-Dichloroethene	96.943	7.21678	1181.12	240.84	6.2741	-3.8257 E-2	6.0461 E-5	0	0	0
cDCE	cis-1,2-Dichloroethene	96.943	7.21953	1290.28	236.887	2.7735 E+1	-1.7832 E-1	2.9328 E-4	0	0	0
tDCE	trans-1,2-Dichloroethene	96.943	7.21356	1244.35	239.497	7.8039	-4.5457 E-2	6.9676 E-4	0	0	0
VC	Vinyl Chloride	62.498	6.91423	911.15	239.8	-4.6670 E+2	1.3479 E+4	1.8523 E+2	-1.3236 E-1	0	0
1,1,1,2-TeCA	1,1,1,2-Tetrachloroethane	167.849	7.03897	1467.16	222.34	2.1790	-1.3966 E-3	2.9328 E-5	0	0	0
1,1,2,2-TeCA	1,1,2,2-Tetrachloroethane	167.849	6.91043	1378.88	197.086	4.8798	-3.0937 E-3	5.2051 E-5	0	0	0
1,1,1,1-TCA	1,1,1,1-Trichloroethane	133.404	7.00718	1253.2	229.624	1.0909	-6.5278 E-3	1.1075 E-5	0	0	0
1,1,2-TCA	1,1,2-Trichloroethane	133.404	7.14357	1457.65	228.099	2.8980	-1.8585 E-2	3.4896 E-5	0	0	0
1,1-DCA	1,1-Dichloroethane	98.959	7.18316	1269.43	237.755	9.4136	-5.7249 E-2	9.1784 E-5	0	0	0
1,2-DCA	1,2-Dichloroethane	98.959	7.29525	1407.85	235.48	1.7915 E+1	-1.1684 E-1	2.0003 E-4	0	0	0
CE	Chloroethane	64.514	7.13047	1097.6	246.009	5.8420 E-1	-1.6863 E-3	9.3949 E-5	-2.5316 E-6	0	0

For all potential contaminants of interest except vinyl chloride, a polynomial correlation [Mackay et al., 2006] is used to obtain the temperature-dependent solubility, as shown in Equation 3. Here, x_p is the mass fraction in weight percent, T is temperature in K (unless the contaminant is CT, CF, DCM, CM, or CE, in which case the temperature is in °C), and A , B , C , D , E , and F are tabulated contaminant-specific correlation coefficients [Mackay et al., 2006], listed in Table 4. Where fewer than six coefficients are given by Mackay et al. [2006], the missing coefficients are set to 0.0. Equation 4 [Yaws, 2003] is used to

calculate the solubility for VC, where x_f is the mass fraction, T is the temperature in K, and A , B , C , and D are tabulated contaminant-specific correlation coefficients [Yaws, 2003] (Table 4). Mass fraction values are converted to mole fraction, x , in Equation 5 by multiplying by the ratio of the molecular weight of water (MW_w , 18.01528 g/mol) to the molecular weight of the contaminant (MW_i , g/mol), also in Table 4.

$$x_p = A + B \cdot T + C \cdot T^2 + D \cdot T^3 + E \cdot T^4 + F \cdot T^5 \quad T \text{ is in K, except use } ^\circ\text{C for CT, CF, DCM, CM, or CE} \quad (3)$$

$$\text{Log}_{10}(x_f) = A + B/T + C \cdot \text{Log}_{10}(T) + D \cdot T \quad T \text{ is in K} \quad (4)$$

$$x = \frac{x_p}{100} \cdot \frac{MW_w}{MW_i} = x_f \cdot \frac{MW_w}{MW_i} \quad (5)$$

As discussed above, the dimensionless Henry's Law constant itself is calculated from the ratio of the vapor pressure (P_{vap}) to the mole fraction (x), with appropriate conversions from units of atm/mol fraction to units of concentration per concentration (i.e., dimensionless). See Sander [1999] for a thorough exposition on distinguishing between multiple representations of the units for the Henry's Law constant. Equation 6 shows the calculation for the unitless Henry's Law constant (H), where ρ_w is the density of water (g/mL), R_{gas} is the gas constant ($0.08205746 \text{ L} \cdot \text{atm} \cdot \text{K}^{-1} \cdot \text{mol}^{-1}$), T is the average subsurface temperature (K), and other quantities were defined above.

$$H = \frac{P_{vap}}{x} \cdot \frac{MW_w}{\rho_w \cdot R_{gas} \cdot T} \cdot \frac{1 \text{ L}}{1000 \text{ mL}} \cdot \frac{1 \text{ atm}}{760 \text{ mmHg}} \quad T \text{ is in K} \quad (6)$$

The unscaled soil gas concentration, C_{gu} , can be scaled to a final concentration based on the site-specific values of the Henry's Law constant (H) and the source strength. If the input included a value for C_{gs} , then Equation 7 is used to calculate the final estimated soil gas contaminant concentration, C_g , at the location directly below the building foundation. If the input included \dot{M}_{src} , then Equation 8 is used to calculate C_g .

$$C_g = C_{gu} \cdot \frac{0.89}{H} \cdot \frac{C_{gs}}{159.0} \quad (7)$$

$$C_g = C_{gu} \cdot \frac{0.89}{H} \cdot \frac{\dot{M}_{src}}{\dot{M}_{sim}} \quad (8)$$

Note that scaling to account for differences in contaminant gas diffusion coefficients is not performed because the differences in coefficient values are small. For the contaminant species in VIETUS, the gas diffusion coefficients average $0.09 \pm 0.015 \text{ cm}^2/\text{s}$ and the range of the differences in gas diffusion coefficients relative to the base case varies from -18% to +48%.

2.4 Estimation of Vapor Intrusion

Vapor intrusion is calculated based on the approach described by Johnson and Ettinger [1991], with the adaptation that the soil gas concentration underneath the building foundation, C_g , is determined from the interpolation and scaling steps described above. Johnson and Ettinger specify equations for the entry rate of vapor contamination into a building and removal of a contaminant as a result of building ventilation (in their equations 14 and 17, respectively). Rearranging their equations to solve for the concentration in the building, C_b , results in Equation 9 below. Several key parameters (Table 2) and one chemical property are required as inputs to this equation.

$$C_b = \frac{Q_s \cdot C_g \cdot \exp\left[\frac{Q_s \cdot L_c}{D_c \cdot A_{inlet}}\right]}{Q_b \cdot \exp\left[\frac{Q_s \cdot L_c}{D_c \cdot A_{inlet}}\right] - Q_b + Q_s} \quad (9)$$

Estimates of appropriate values for the Equation 9 input parameters (Q_b , A_{inlet} , L_c , and Q_s) can be obtained from relevant calculations (some of which are left for the user to complete external to the VIETUS software in the interest of streamlined inputs) and from guidance/data in U.S. Environmental Protection Agency (EPA) reports [EPA, 2004; 2012]. The EPA's *User's Guide for Evaluating Subsurface Vapor Intrusion into Buildings* [EPA, 2004] provides insight into application of the Johnson and Ettinger model, including relevant calculations, appropriate ranges of parameters, and selected default values. Table 5 lists relevant ranges and default values from EPA [2004]. The 2012 Vapor Intrusion Database [EPA, 2012] provides a data set from which inferences can be drawn regarding "typical" values observed for various vapor intrusion related parameters.

Table 5. Typical ranges of parameter values for residential buildings taken from EPA [2004] guidance

Parameter	Units	Nominal Range EPA 2004	EPA Recommended Default Value
<i>building footprint</i>	m ²	80 – 225	100
<i>mixing height</i>	m	2.13 – 4.88	2.44 (slab) 3.66 (basement)
<i>air exchange rate</i>	day ⁻¹	2.4 – 36	6
η (= A_c / A_b)	—	0.0001 – 0.0019	0.000344 (slab) 0.00022 (basement)
w_c	m	0.0005 – 0.01	0.001
Q_s	m ³ /d	1.44 – 14.4	7.2
k_v	m ²	1.0 E-10 – 1.0 E-16	1.0 E-12 (fine sand)
ΔP	Pa	0 – 20	4
L_c	m	—	0.1
dz	m	—	0.15 (slab) 2.0 (basement)

EPA [2004] guidance for the foundation/wall thickness simply recommends a value of 0.1 m. However, for flexibility, the VIETUS software allows values up to 0.61 m.

The building ventilation rate, Q_b , is a user input that can be estimated (externally by the user) from other quantities using Equation 10. Based on EPA [2004] information (also listed in Table 5), a typical residential building would have a ventilation rate in the range of 1500 to 2400 m³/d. The VIETUS software suggests a range of 1200 to 10,000 m³/d, but allows the user to specify a value up to 80,000 m³/d to allow flexibility for different building configurations.

$$Q_b = (\text{footprint area}) \cdot (\text{mixing height}) \cdot (\text{air exchange rate}) \quad (10)$$

The A_{inlet} term of Equation 9 represents the area through which vapor can migrate into the building. For the porous foundation case, this area is the sub-grade surface area of the foundations, A_b , calculated as shown in Equation 11. For the case of foundation cracks, the area of the cracks, A_c , can be estimated either from the crack ratio, η , or from a nominal crack width, w_c , and a cumulative crack length, x_c , as shown in Equations 12 and 13, respectively (and where r_c is the nominal crack radius). A common assumption is that the primary cracks are at the joints between the foundation floor and the walls. Such a “perimeter crack” would have a total length (x_c) equal to the building perimeter, as calculated from the building width (W_b) and length (L_b) in Equation 14. The calculations in Equations 11 to 14 are used in the VIETUS software to provide defaults based on the secondary input parameter values, though the user can override the default calculations by entering a site-specific number. Permissible ranges are not applied directly to A_{inlet} , A_b , or A_c , though constraints on η , W_b , L_b , and/or w_c will constrain the calculated values for the area. In addition, a limit related to calculation of the Q_s value is imposed on A_c , as discussed below.

$$A_b = dx \cdot dy + 2 \cdot dx \cdot dz + 2 \cdot dy \cdot dz \quad (11)$$

$$A_c = \eta \cdot A_b \quad (12)$$

$$A_c = w_c \cdot x_c = 2 \cdot r_c \cdot x_c \quad (13)$$

$$x_c = 2 \cdot W_b + 2 \cdot L_b \quad (14)$$

The gas flow rate into the building from the surrounding soil can either be directly input or can be estimated using the approach described by Johnson and Ettinger [1991] in their sample calculations for the scenario of vapor intrusion through cracks in the foundation. Johnson and Ettinger assumed that the cracks were filled with dust/dirt that was similar in nature (e.g., porosity, moisture content) to the soil underlying the foundation. As a simplification, the approach proposed by Nazaroff [1988] was used to estimate Q_s from a total crack length (e.g., representing the total perimeter for the floor/wall seam), the crack width, soil properties, and building under-pressurization. This approach to estimating gas flow into the building is based on an idealized model of cracks at the floor/wall seams, where the crack is a long cylinder of specified radius. Taking the crack radius, r_c , to be half of the quotient of the area of the cracks, A_c , divided by the cumulative crack length, x_c , the estimate of Q_s is determined from Equation 15 (a variant of Johnson and Ettinger’s equation 24). The μ_g parameter is the viscosity of air at the subsurface temperature, π has the standard meaning of the constant, and the other parameters for this equation are identified in Table 2. This method of estimating Q_s is presented as an optional approach that may be selected if the assumptions are suitable for a given site, or which can be neglected in favor of direct entry of Q_s (e.g., for a porous foundation scenario or based on measurements from tracer tests).

$$Q_s = \frac{2 \cdot \pi \cdot \Delta P \cdot k_v}{\mu_g} \cdot \frac{x_c}{\ln(4 \cdot dz \cdot x_c) - \ln(A_c)} \quad (15)$$

As with the Q_b calculation, information from EPA documents is used as a guide for appropriate ranges of secondary input parameters. The air viscosity is a simple lookup/interpolation calculation based on published data [Lemmon, 2014]. The permeability of soil adjacent to the foundation is very site-specific, but EPA [2004] provides a range (see Table 5) and recommends a default value of 1.0E-12 m², representing fine sand. Typical ranges of building under-pressure are also provided by EPA [2004] (Table 5). The EPA guidance is also used to constrain Q_s values themselves. EPA [2004] suggests that a range from 1.44 to 14.4 m³/d is reasonable, while a review of data [EPA, 2012] indicates that Q_s is

typically 3% or less of the building ventilation rate, Q_b . The VIETUS software suggests an upper limit of $(x_c/40) \cdot 15$ to allow scaling to larger building sizes. However, Q_s values as large as 6% of Q_b are permitted (which is twice the observed ratio of Q_s/Q_b).

The final parameter used in Equation 9 (and not listed in Table 2) for the vapor intrusion estimate is the gas diffusion coefficient, D_c , describing vapor diffusion of the contaminant through the porous media of the cracks or building foundation. Using the same Millington-Quirk approach as taken by Johnson and Ettinger [1991], the value of D_c can be calculated from Equation 16. Here, $\theta_{c,g}$ is the gas porosity of the cracks/foundation, $\theta_{c,total}$ is the total porosity within the cracks/foundation, and D_a is the diffusion coefficient in air (m^2/day) for the contaminant of interest. The EPA [2004] guidance takes the crack moisture content to be “dry” though Johnson and Ettinger [1991] used a value similar to the underlying soil in their example. However, the Johnson and Ettinger model only accounts for gas diffusion and convective vapor movement into a building, so the VIETUS software will flag the $\theta_{c,g}$ if it is less than 50% of the total crack/foundation porosity.

$$D_c = \frac{D_a \cdot \theta_{c,g}^{\frac{10}{3}}}{\theta_{c,total}^2} \quad (16)$$

The diffusion coefficient in air, which is used to determine a gas diffusion coefficient for the porous cracks/foundation, can be calculated from Equation 17 using the tabulated contaminant-specific correlation coefficients listed in Table 6 [Yaws, 2003].

$$D_a = (A + B \cdot T + C \cdot T^2) \cdot (86400 / 100^2) \quad \text{T is in K} \quad (17)$$

Table 6. Tabulated correlation coefficients for calculating the gas diffusion coefficient for contaminants of interest, from Yaws [2003]

Contaminant Abbrev.	Contaminant	Correl. Coef. for Calculating Gas Diffusion Coef.		
		A	B	C
CT	Carbon Tetrachloride	-4.1620 E-2	2.5749 E-4	5.3598 E-7
CF	Chloroform	-4.9960 E-2	2.8829 E-4	5.9407 E-7
DCM	Dichloromethane	-5.6860 E-2	3.3534 E-4	6.8151 E-7
CM	Chloromethane	-6.9250 E-2	4.2133 E-4	8.2225 E-7
PCE	Tetrachloroethene	-3.6840 E-2	2.3847 E-4	5.1123 E-7
TCE	Trichloroethene	-4.1270 E-2	2.6580 E-4	5.5704 E-7
1,1-DCE	1,1-Dichloroethene	-4.5030 E-2	2.9721 E-4	6.0085 E-7
cDCE	cis-1,2-Dichloroethene	-4.6220 E-2	3.0091 E-4	6.1981 E-7
tDCE	trans-1,2-Dichloroethene	-4.6380 E-2	3.0373 E-4	6.2044 E-7
VC	Vinyl Chloride	-5.4240 E-2	3.6658 E-4	7.2028 E-7
1,1,1,2-TeCA	1,1,1,2-Tetrachloroethane	-3.6290 E-2	2.2950 E-4	4.9507 E-7
1,1,2,2-TeCA	1,1,2,2-Tetrachloroethane	-4.0420 E-2	2.2899 E-4	4.9882 E-7
1,1,1-TCA	1,1,1-Trichloroethane	-4.5040 E-2	2.5770 E-4	5.3553 E-7
1,1,2-TCA	1,1,2-Trichloroethane	-4.4400 E-2	2.5339 E-4	5.4055 E-7
1,1-DCA	1,1-Dichloroethane	-4.7450 E-2	2.8979 E-4	5.9566 E-7
1,2-DCA	1,2-Dichloroethane	-4.8920 E-2	2.8847 E-4	6.0315 E-7
CE	Chloroethane	-5.5930 E-2	3.4520 E-4	6.8934 E-7

Equations 9 and 15 both include terms that can cause the calculations to fail. Thus, the set of parameters that comprise these terms are constrained to avoid calculation failure. For Equation 15, the ratio $4 \cdot dz \cdot x_c / A_c$ must be greater than 1. The user can avoid this calculational constraint by directly entering a

Q_s value (setting the secondary parameters x_c and A_c to empty values). For Equation 9, the $(Q_s \cdot L_c)/(D_c \cdot A_{inlet})$ term must be of a magnitude to avoid failure of the exponential function. If the site-specific configuration, as entered into the VIETUS software, results in a failure due to this term (i.e., for convection dominated transport through the foundation cracks), then the user is referred to Johnson and Ettinger [1991], who discuss an alternate formulation for their attenuation factor (in their equation 22).

2.5 Limitations and Assumptions

The procedure described in this report provides an *estimate* of vapor intrusion based on user-defined inputs and a set of constraints/assumptions. The usefulness of such estimates must be evaluated for a specific site, considering whether the constraints/assumptions are appropriate. One element to consider is the uncertainty of input parameter values. While input parameters are often not known precisely, a sensitivity analysis can readily be conducted with the VIETUS software to assess the potential impact of reasonable variation in specific input parameters on the estimated vapor intrusion results. Another aspect to consider is the relevance of factors outside the scope of the calculational approach used in the VIETUS software, which constrains the scenarios for which the estimates are suitable. Other evaluation approaches (perhaps in conjunction with estimates from the VIETUS software) may be needed to consider factors such as the degree of source depletion over time, adsorption, biological transformation, other physical attenuation mechanisms, multiple sources, sources in the groundwater, and variation in recharge/infiltration through the vadose zone source. In addition to constraints on factors include in the calculational approach, the appropriateness of simplifying assumptions used in the approach should be considered with respect to the site-specific conditions. For instance, the generalized conceptual model used in the approach is appropriate for sites where vapor-phase transport dominates contaminant movement.

It is important to understand the scope of the calculation approach/tool presented here. Figure 1 depicts the vapor-phase diffusion from the current vadose zone source and the resulting steady-state distribution of contamination in the vadose zone and the associated contamination in groundwater. VIETUS is not configured to address vapors that arise either solely from groundwater plumes (i.e., where contamination was released directly to groundwater or where a vadose zone source is not currently present) or from groundwater contamination resulting from a historically stronger vadose zone source. This tool is intended to supply information to support a decision about SVE disposition relative to diminishing returns in remediation of a vadose zone contaminant source (i.e., “If we stop SVE now, would we expect a vapor intrusion issue from the remaining source?”).

Specific Limitations and Assumptions:

- Vapor-phase transport dominates contaminant movement in the vadose zone source.
- The specific site can be suitably represented by the generalized conceptual site model.
- The contaminant source can be represented as single source area in the vadose zone within a square footprint of specified size and thickness. Note that it may be appropriate for a cluster of separate sources to be represented as a single source with respect to vapor transport (see Truex et al. [2013] and the discussion of the generalized conceptual model in Section 2.0).
- The contaminant source strength can be represented as a constant vapor-phase contaminant concentration or a mass discharge of contaminant that results in a steady-state distribution of contaminant in the subsurface.

- Simulations were run to obtain steady-state concentration distributions in the gas and aqueous phases throughout the computational domain.
- There are no additional sources in the vadose zone or groundwater.
- The subsurface can be approximated as a homogeneous material (i.e., is not layered or heterogeneous) with uniform properties (temperature, vadose zone moisture content, bulk density, porosity). Note that some types of heterogeneity may have minimal impact on vapor transport and can be approximated as homogeneous (see Truex et al. [2013] and the discussion of the generalized conceptual model in Section 2.0).
- The transverse transport of contaminant (perpendicular to the numerical model x-axis) is symmetrical, so only half of a model domain in the y-axis direction need be modeled. Note that the direction of groundwater flow is parallel to the numerical model x-axis.
- Extrapolation outside the bounds of the model domain or bounds of parameter key values is not allowed. See Table 1 and Table 2 for lists of the permissible ranges for parameters.
- Approximations inherent in using linear interpolation between key values are small relative to the accuracy needed for the estimate.
- Differences in contaminant-specific gas phase diffusion coefficients are small enough to neglect when scaling the soil-gas concentration results from the pre-modeled scenarios.
- Soil gas concentration data from the simulations consists of values greater than 1 ng/L (values below that cutoff are ignored).
- Foundations do not extend more than 4 m below ground surface and ½ m depth increments provide sufficient resolution for specifying a site scenario.
- Recharge is assumed to be low, such that use of simulation results based on a recharge of 0.4 cm/yr is appropriate to represent conditions where vapor-phase transport in the vadose zone dominates (see also the discussion below).
- Vapor intrusion is based on an adaptation of the Johnson and Ettinger [1991] model. Numerical simulation results are used for the subsurface transport component while the Johnson and Ettinger model is applied to determine the entry rate of contaminant into the building (as driven by building ventilation) and the associated building concentration for the contaminant. This decoupling of diffusive flux in the subsurface and the rate of vapor intrusion will result in vapor intrusion estimates that differ from the full Johnson and Ettinger model.
- The distribution of soil-gas concentration in the subsurface is a result of diffusive transport and does not account for advection (from barometric pumping, density effects, or induced by the building under-pressurization. However, the EPA [2004] note that the zone of influence for advective contaminant flow due to vapor intrusion is expected to be limited to a region immediately adjacent to the building foundation.
- A single soil-gas contaminant concentration is used to determine the concentration in the building.
- Vapor intrusion occurs through either cracks (which could be floor/wall seams) or a porous foundation.

- Cracks are assumed to be filled with dust/dirt with sufficient air-filled porosity to allow vapor intrusion into the building.
- The estimate of gas flow into the building based on secondary vapor intrusion parameters assumes an idealized model of cracks at the floor/wall seams, where the crack is a long cylinder of specified radius [Johnson and Ettinger, 1991]. However, the user can externally determine this gas flow into the building and can input a specific value.
- Gas flow into a building for a porous foundation occurs through the entire subsurface area of the foundation [Johnson and Ettinger, 1991].
- The temperature dependence of the Henry's Law constant is determined as suggested by Brennan et al. [1998] using vapor pressure and solubility values.
- The Antoine correlation [Yaws et al., 2009] is suitable for determining vapor pressure at a specified temperature.
- The correlations of Mackay et al. [2006] and Yaws [2003] are suitable for determining solubility at a specified temperature.
- The correlations of Yaws [2003] are suitable for determining the gas diffusion at a specified temperature.

The impact of recharge on the soil-gas contaminant concentration in the vadose zone is likely to be complicated. Recharge affects the mass flux from the vadose zone source into the groundwater. Once in the groundwater, contaminant mass can be transported downgradient and then volatilize back into the vadose zone at a distance from the source. This effect could occur due to higher recharge, a strong source close to the groundwater, or a source within the groundwater. Regardless, the relationships are complicated and it is possible that a significant amount of additional simulations would be required to understand the behavior. Thus, the VIETUS software currently focuses only on estimating the impact of the vadose zone source on vapor intrusion for a low value of recharge where vapor-phase transport in the vadose zone dominates. Site-specific simulations should be investigated for cases where recharge is more significant (or where a significant source within the groundwater exists).

3.0 Example Calculation

To illustrate the procedure for estimating the soil gas and building contaminant concentrations, this example walks through the calculations for the scenarios shown in Table 7. These scenarios represent the compiled set of input data for three variants (Cases A, B, and C), which differ in the way that the source strength is specified, the way in which the crack area is calculated, the method for input of Q_s , and the lateral location of the building. Case A uses a crack width to estimate the area of cracks and has a directly specified value of Q_s . Case B uses a crack ratio to estimate the area of cracks and Q_s is from the default calculation. Case C is similar to Case B, but the source strength is specified as a mass discharge, the lateral location of the building is closer to the source, and the under-pressure is halved.

Table 7. User input for the scenario variants applied in the example calculations for estimation of the soil gas concentrations and vapor intrusion

User Input – Source/Transport Parameters					
	Scenario Name:	—	Case A	Case B	Case C
	Contaminant:	—	TCE	TCE	TCE
T	Temperature:	[°C]	20	20	20
ω	Avg. Moisture Content:	[wt %]	2.825	2.825	2.825
VZT	Vadose Zone Thickness:	[m]	20	20	20
L1	Depth to Top of Source:	[m]	5.85	5.85	5.85
z	Source Thickness:	[m]	3.5	3.5	3.5
w (= l)	Source Width (= Length):	[m]	15.8	15.8	15.8
q	GW Darcy Velocity:	[m/day]	0.165	0.165	0.165
	Source Strength Input Type:	—	Gas Concentration	Gas Concentration	Mass Discharge
C_{gs}	Source Gas Concentration:	[ppmv]	159	159	
\dot{M}_{src}	Source Mass Discharge:	[g/day]			58
Total porosity = 0.3, dry bulk density = 1.855 g/mL, and recharge = 0.4 cm/yr.					
User Input – Vapor Intrusion Parameters					
dx	Longitudinal Distance to Building:	[m]	50	50	20
dy	Transverse Distance to Building:	[m]	10	10	20
dz	Depth of Basement/Foundation:	[m]	4	4	4
L_c	Foundation/Wall Thickness:	[m]	0.1	0.1	0.1
Q_b	Building Ventilation Rate:	[m ³ /day]	2000	2000	2000
User Input – Vapor Intrusion Parameters (directly specified or calculated from 2 ² parameters)					
Q_s	Gas Flow Into Building from Soil:	[m ³ /day]	8.0	1.862	0.931
A_{inlet}	Inlet Area (Cracks or "Pores"):	[m ²]	0.6	0.44	0.44
$\theta_{c, total}$	Total Porosity within Crack/Fndn:	[--]	0.3	0.3	0.3
$\theta_{c, g}$	Gas-Filled Porosity for Cracks/Fndn:	[--]	0.225	0.225	0.225
Need to ↑ A_c or ↓ Q_s Need to ↑ A_c or ↓ Q_s Need to ↑ A_c or ↓ Q_s					
User Input – Secondary Vapor Intrusion Parameters (for deriving Q_s and A_{inlet})					
	Vapor Intrusion Path Type:	—	Cracks	Cracks	Cracks
W_b	Building Width:	[m]	10	10	10
L_b	Building Length:	[m]	20	20	20
ΔP	Building Underpressure:	[Pa]		8	4
k_v	Near-Building Soil Gas Permeability:	[m ²]		1.00E-12	1.00E-12
	A_c from Crack Ratio/Width/Direct:	—	Width	Ratio	Ratio
η	Crack Ratio (A_c / A_b):	[--]		0.001	0.001
w_c	Crack Width:	[m]	0.01		
x_c	Cumulative Lateral Crack Length:	[m]	60	60	60
A_c	Total Area of Foundation Cracks:	[m ²]	0.6	0.44	0.44

The calculation procedure begins by performing the interpolation, which is done in two phases: a spatial interpolation phase and a phase to interpolate between key-value scenarios. A key-value scenario is defined as a specific permutation of key values for the six source/transport parameters (RSP , q , SA , VZT , STR , and S_r , as discussed in Table 1) that exhibit a nonlinear concentration response.

The first phase interpolates soil gas data between numerical model grid cell centers and model layers to obtain a soil gas concentration for the arbitrary lateral location (dx and dy) and depth of basement/foundation (dz) that are specified in the inputs. Figure 6 depicts both a set of concentrations from the simulation results (using the 26th key-value scenario of parameters for Cases A and B as an example) and the process of interpolating in three dimensions to obtain the concentration at the point of interest (marked with the star). Concentrations at grid cell centers (dots) from the layer above and the layer below the depth of interest are interpolated to obtain four “corner” concentrations (squares) at the depth of interest. Then a bilateral interpolation is performed to determine the soil gas concentration, C_{sim} , at the lateral location of interest (star). This spatial interpolation process is repeated to supply the 64 C_{sim} values used in the second phase of interpolation.

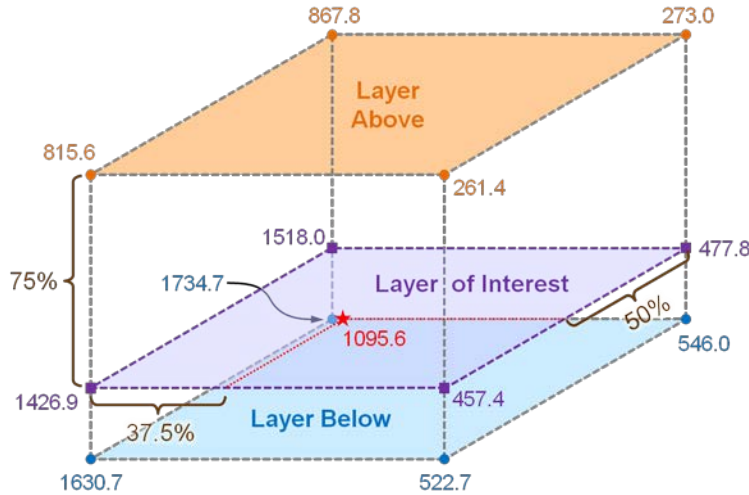


Figure 6. Example of the spatial interpolation from numerical grid cell centers (dots) to the location of interest (denoted with a star) within the bounds of those cell centers. Interpolation is done vertically first to obtain the four corners of the layer of interest (squares), then done laterally to find the soil gas concentration at the point of interest.

The second phase of interpolation involves interpolating between key-value scenarios for the RSP , q , SA , VZT , STR , and S_r parameters to match the site-specific conditions. The user directly specifies the site-specific values of VZT and q , while values of RSP , SA , STR , and S_r (i.e., the converted value of ω , as discussed in the footnotes to Table 1) are calculated from other input parameters. Table 8 lists the site-specific values of these six parameters for the three example cases. Each of the 64 key-value scenarios between which the interpolation occurs, represents a simulation with parameters at key values above or below (or perhaps equal to) the user-specified parameter values. Table 9 lists the C_{sim} values for Cases A and B and the subsequent interpolation results for the six parameters to arrive at the final soil gas concentration, C_{gu} . Case C has different values because of the different spatial location specified.

Table 8. Parameter values for the example cases that are used in the second phase of interpolation

	Scenario Name:	—	Case A	Case B	Case C
S_r	Residual Saturation:	[--]	0.175	0.175	0.175
STR	Source Thickness Ratio:	[--]	0.175	0.175	0.175
VZT	Vadose Zone Thickness:	[m]	20	20	20
SA	Areal Footprint of Source:	[m ²]	250	250	250
q	GW Darcy Velocity:	[m/day]	0.165	0.165	0.165
RSP	Relative Source Position:	[--]	0.55	0.55	0.55

Table 9. Sequential interpolation to determine C_{gu} (ppbv) for Cases A and B of the example; starting with the 64 C_{sim} values, results of linear interpolations between adjacent pairs of values are shown in the columns, from left to right, with the rightmost column showing the value of C_{gu}

Key-Value Scenario (RSP, q, SA, VZT, STR, Sr)	C_{sim} Value (ppbv)	After RSP Interpolation	After q Interpolation	After SA Interpolation	After VZT Interpolation	After STR Interpolation	After Sr Interpolation
0.1, 0.03, 100, 10, 0.1, 0.05	28.0	44.7	64.2	128.8	485.6	531.3	617.5
1.0, 0.03, 100, 10, 0.1, 0.05	61.3						
0.1, 0.3, 100, 10, 0.1, 0.05	52.7	83.7	193.8	842.4	576.9	703.8	617.5
1.0, 0.3, 100, 10, 0.1, 0.05	114.8						
0.1, 0.03, 400, 10, 0.1, 0.05	97.2	136.6	580.4	1049.5	747.3	1187.9	617.5
1.0, 0.03, 400, 10, 0.1, 0.05	176.1						
0.1, 0.3, 400, 10, 0.1, 0.05	179.3	251.0	1105.7	1333.5	945.4	1239.6	617.5
1.0, 0.3, 400, 10, 0.1, 0.05	322.9						
0.1, 0.03, 100, 30, 0.1, 0.05	339.5	582.7	766.8	1531.7	1049.5	1484.3	617.5
1.0, 0.03, 100, 30, 0.1, 0.05	826.6						
0.1, 0.3, 100, 30, 0.1, 0.05	334.0	578.1	1109.1	1822.3	1187.9	2062.5	617.5
1.0, 0.3, 100, 30, 0.1, 0.05	823.0						
0.1, 0.03, 400, 30, 0.1, 0.05	775.9	1109.1	1333.5	1331.7	945.4	1239.6	617.5
1.0, 0.03, 400, 30, 0.1, 0.05	1443.3						
0.1, 0.3, 400, 30, 0.1, 0.05	763.3	1102.4	156.1	764.4	660.3	703.8	617.5
1.0, 0.3, 400, 30, 0.1, 0.05	1442.5						
0.1, 0.03, 100, 10, 0.25, 0.05	22.2	36.5	52.9	104.4	576.9	531.3	617.5
1.0, 0.03, 100, 10, 0.25, 0.05	50.8						
0.1, 0.3, 100, 10, 0.25, 0.05	42.4	69.4	156.1	104.4	576.9	531.3	617.5
1.0, 0.3, 100, 10, 0.25, 0.05	96.5						
0.1, 0.03, 400, 10, 0.25, 0.05	70.7	108.8	766.8	1049.5	747.3	1187.9	617.5
1.0, 0.03, 400, 10, 0.25, 0.05	147.0						
0.1, 0.3, 400, 10, 0.25, 0.05	132.6	203.3	1333.5	1331.7	945.4	1239.6	617.5
1.0, 0.3, 400, 10, 0.25, 0.05	274.3						
0.1, 0.03, 100, 30, 0.25, 0.05	443.8	769.2	766.8	1531.7	1049.5	1484.3	617.5
1.0, 0.03, 100, 30, 0.25, 0.05	1095.6						
0.1, 0.3, 100, 30, 0.25, 0.05	436.4	764.4	1109.1	1822.3	1187.9	2062.5	617.5
1.0, 0.3, 100, 30, 0.25, 0.05	1093.4						
0.1, 0.03, 400, 30, 0.25, 0.05	854.9	1335.4	1333.5	1331.7	945.4	1239.6	617.5
1.0, 0.03, 400, 30, 0.25, 0.05	1817.4						
0.1, 0.3, 400, 30, 0.25, 0.05	842.5	1331.7	156.1	764.4	660.3	703.8	617.5
1.0, 0.3, 400, 30, 0.25, 0.05	1822.3						
0.1, 0.03, 100, 10, 0.1, 0.3	76.6	120.9	188.0	375.2	660.3	703.8	617.5
1.0, 0.03, 100, 10, 0.1, 0.3	165.4						
0.1, 0.3, 100, 10, 0.1, 0.3	160.3	255.0	563.2	104.4	576.9	531.3	617.5
1.0, 0.3, 100, 10, 0.1, 0.3	350.0						
0.1, 0.03, 400, 10, 0.1, 0.3	261.1	363.9	766.8	1049.5	747.3	1187.9	617.5
1.0, 0.03, 400, 10, 0.1, 0.3	467.1						
0.1, 0.3, 400, 10, 0.1, 0.3	542.1	762.5	1333.5	1331.7	945.4	1239.6	617.5
1.0, 0.3, 400, 10, 0.1, 0.3	983.7						
0.1, 0.03, 100, 30, 0.1, 0.3	385.3	670.0	766.8	1531.7	1049.5	1484.3	617.5
1.0, 0.03, 100, 30, 0.1, 0.3	955.7						
0.1, 0.3, 100, 30, 0.1, 0.3	358.0	635.2	1109.1	1822.3	1187.9	2062.5	617.5
1.0, 0.3, 100, 30, 0.1, 0.3	913.4						
0.1, 0.03, 400, 30, 0.1, 0.3	877.4	1268.0	1333.5	1331.7	945.4	1239.6	617.5
1.0, 0.03, 400, 30, 0.1, 0.3	1659.8						
0.1, 0.3, 400, 30, 0.1, 0.3	817.0	1211.1	156.1	764.4	660.3	703.8	617.5
1.0, 0.3, 400, 30, 0.1, 0.3	1606.5						
0.1, 0.03, 100, 10, 0.25, 0.3	60.7	99.2	155.9	306.7	747.3	1187.9	617.5
1.0, 0.03, 100, 10, 0.25, 0.3	137.8						
0.1, 0.3, 100, 10, 0.25, 0.3	128.8	212.6	580.4	1105.7	842.4	531.3	617.5
1.0, 0.3, 100, 10, 0.25, 0.3	296.7						
0.1, 0.03, 400, 10, 0.25, 0.3	191.1	292.6	766.8	1049.5	747.3	1187.9	617.5
1.0, 0.03, 400, 10, 0.25, 0.3	394.5						
0.1, 0.3, 400, 10, 0.25, 0.3	403.4	623.9	1109.1	1822.3	1187.9	2062.5	617.5
1.0, 0.3, 400, 10, 0.25, 0.3	845.0						
0.1, 0.03, 100, 30, 0.25, 0.3	503.3	888.2	869.2	1187.9	747.3	1187.9	617.5
1.0, 0.03, 100, 30, 0.25, 0.3	1274.3						
0.1, 0.3, 100, 30, 0.25, 0.3	469.7	850.2	1333.5	1331.7	945.4	1239.6	617.5
1.0, 0.3, 100, 30, 0.25, 0.3	1231.9						
0.1, 0.03, 400, 30, 0.25, 0.3	966.2	1531.7	1508.0	1484.3	2062.5	617.5	617.5
1.0, 0.03, 400, 30, 0.25, 0.3	2099.0						
0.1, 0.3, 400, 30, 0.25, 0.3	907.9	1484.3	1508.0	1484.3	2062.5	617.5	617.5
1.0, 0.3, 400, 30, 0.25, 0.3	2062.5						

The first column of Table 9 lists the C_{sim} values from the spatial interpolation for Cases A and B. Each subsequent column is determined by applying the linear interpolation of Equation 1 to adjacent values. The key RSP values (Table 1) are 0.1 and 1.0, because the site-specific RSP value is 0.55 (Table 8). The first pair of C_{sim} values in Table 9 corresponds to those two key values of RSP (for the same key values of q , SA , VZT , STR , and S_r), so interpolation for RSP can be applied as:

$$\left[\frac{0.55 - 0.1}{1.0 - 0.1} \right] \cdot (61.3 - 28.0) + 28.0 = 44.7 \text{ ppbv}$$

This same interpolation process is performed for the remaining pairs of C_{sim} values to get the intermediate interpolation results in the second column of Table 9. Pairs of values from the second column are then interpolated to obtain concentration values for the user-specified q value of 0.165 m/day (Table 8). The key q values (Table 1) above and below the site-specific q are 0.03 and 0.3 m/day. The interpolation of the first pair of concentrations in the second column thus gives:

$$\left[\frac{0.165 - 0.03}{0.3 - 0.03} \right] \cdot (44.7 - 83.7) + 83.7 = 64.2 \text{ ppbv}$$

This process continues in the same fashion for pairs of values with interpolation between key values to the site-specific conditions for the q , SA , VZT , STR , and S_r parameters. The results of these sequential linear interpolations are shown in Table 9, with the final interpolation providing the C_{gu} value of 617.5 ppbv (for Cases A and B).

For Case C of the example, interpolation is required to determine the source mass discharge, \dot{M}_{sim} , corresponding to the site-specific parameter values. This value is used in the scaling process. Interpolation to determine \dot{M}_{sim} does not involve the first phase of spatial interpolation (because it pertains to the defined source), but does involve the second phase to interpolate to the site-specific conditions for the RSP , q , SA , VZT , STR , and S_r parameters in a process parallel to that shown in Table 9. The initial values of mass discharge, from which the 64 values are drawn, are tabulated in the VIETUS software (see the SVEET documentation [Truex et al., 2013] for a list of all mass discharge values). For Case C, the resultant \dot{M}_{sim} is 58.3 g/day and the C_{gu} value is 1425.9 ppbv.

Once C_{gu} (and \dot{M}_{sim} , if needed) are determined, the next step is to apply scaling factors for the two parameters (Henry's Law Constant and source strength) where concentration exhibits a linear response.

The vapor pressure and solubility for trichloroethene at 20 °C are calculated using contaminant-specific correlations in Equations 2 and 3 (with conversion of solubility to mole fraction based on Equation 5):

$$P_{vap} = 10^{[6.87981 - 1157.83 / (20.0 + 202.58)]} = 47.6376 \text{ mm Hg}$$

$$x_p = [1.4049 - 0.0082223 \cdot (20.0 + 273.15) + 0.000013218 \cdot (20.0 + 273.15)^2] / 100 = 0.13045$$

$$x = (0.13045 / 100) \cdot (18.01528 / 131.387) = 1.7886 \times 10^{-4}$$

These results are used with Equation 6 to obtain the dimensionless value for the Henry's Law constant:

$$\frac{47.6376}{0.00017886} \cdot \frac{18.01528}{0.9982 \cdot 0.08205746 \cdot 293.15} \cdot \frac{1}{1000} \cdot \frac{1}{760} = 0.263$$

For Cases A and B of the example, Equation 7 is applied to obtain the final estimated soil gas contaminant concentration, C_g , at the specified location beneath the building foundation. For Case C, Equation 8 is applied to obtain C_g because the source strength is specified as a mass discharge. These final calculations give the following results:

$$\text{Cases A \& B: } 617.5 \cdot \frac{0.89}{0.263} \cdot \frac{159.0}{159.0} = 2090 \text{ ppbv}$$

$$\text{Case C: } 1425.9 \cdot \frac{0.89}{0.263} \cdot \frac{58}{58.3} = 4798 \text{ ppbv}$$

Given the soil gas concentration beneath the building foundations, the final step is to generate the estimate of the contaminant concentration in the building due to vapor intrusion. The diffusion coefficient in air for TCE at 20 °C is calculated with the correlation formula of Equation 17 and associated constants in Table 6:

$$D_a = -4.127\text{E-}2 + (2.658\text{E-}4)(293.15) + (5.5704\text{E-}7)(293.15)^2 = 0.0845 \text{ cm}^2/\text{s} = 0.73025 \text{ m}^2/\text{day}$$

The diffusion coefficient through cracks in the foundation is then calculated with Equation 16:

$$D_c = \frac{0.73025 \cdot (0.225)^{\frac{10}{3}}}{0.3^2} = 0.0562 \text{ m}^2 / \text{day}$$

The area through which vapor intrusion occurs (A_{inlet}) is the area of the cracks (A_c) for the three cases considered here. For Case A, a crack width is specified and the crack area is calculated as the crack width times the cumulative lateral crack length (i.e., the building perimeter). For Cases B and C, the crack area is estimated based on a crack ratio and the total surface area of the below-ground walls and floor.

$$\text{Case A: } A_{inlet} = A_c = w_c \cdot x_c = w_c \cdot (2 \cdot W_b + 2 \cdot L_b) = (0.01) (60) = 0.6 \text{ m}^2$$

$$\text{Cases B \& C: } A_{inlet} = A_c = \eta \cdot A_b = \eta \cdot (2 \cdot W_b \cdot dz + 2 \cdot L_b \cdot dz + W_b \cdot L_b) = (0.001) (440) = 0.44 \text{ m}^2$$

Case A uses a directly specified value for the gas flow into the building. Cases B and C use Equation 15 to estimate Q_s . For Case B the calculation is:

$$Q_s = \frac{2 \cdot \pi \cdot 8 \cdot 10^{-12}}{2.107 \times 10^{-10}} \cdot \frac{60}{\ln(4 \cdot 4 \cdot 60) - \ln(0.44)} = 1.862 \text{ m}^3 / \text{day}$$

The same calculation with Case C parameter values gives $Q_s = 0.931$ (because the building under-pressure is half as much).

Having defined all key values, Equation 9 can be applied to determine the estimate for the contaminant concentration in the building. First calculating the term inside the exponential function:

$$\begin{aligned} \frac{Q_s \cdot L_c}{D_c \cdot A} &= [(0.1) (8)] / [(0.6) (0.0562)] &= 23.72 && \text{for Case A} \\ &= [(0.1) (1.862)] / [(0.44) (0.0562)] &= 7.53 && \text{for Case B} \\ &= [(0.1) (0.931)] / [(0.44) (0.0562)] &= 3.76 && \text{for Case C} \end{aligned}$$

Then, completing the calculation for each separate example case, the contaminant concentration in the building is estimated to be:

$$C_b = \frac{8 \cdot 2090 \cdot \exp(23.72)}{2000 \cdot \exp(23.72) - 2000 + 8} = 8.4 \text{ ppbv} \quad \text{for Case A}$$

$$C_b = \frac{1.862 \cdot 2090 \cdot \exp(7.53)}{2000 \cdot \exp(7.53) - 2000 + 1.862} = 2.0 \text{ ppbv} \quad \text{for Case B}$$

$$C_b = \frac{0.931 \cdot 4798 \cdot \exp(3.76)}{2000 \cdot \exp(3.76) - 2000 + 0.931} = 2.3 \text{ ppbv} \quad \text{for Case C}$$

4.0 VIETUS User Guide

For user convenience, the calculational procedure for estimating a soil-gas contaminant concentration in the vadose zone and the associated vapor intrusion concentration (described in Section 2.0 and illustrated in Section 3.0) has been implemented in a spreadsheet software tool. The VIETUS software allows the user to easily enter data and calculate the estimated soil gas and building concentrations for one or more scenarios conforming to the generalized conceptual model described in Section 2.0. The system requirements, installation, user interface, and application of the VIETUS software are described in the sections below.

4.1 System Requirements

The following hardware and software are required to use the VIETUS software:

- Personal computer based on Intel® IA-32 or Intel® 64 processor architectures,
- Microsoft® Windows® XP or Microsoft® Windows® 7 operating system,
- Microsoft® Excel® 2007 or Excel® 2010

The VIETUS software should also work with Windows® 8, Windows® 10, Excel® 2013, and Excel® 2016, but these versions have not been specifically tested. Use of the operating system/Excel versions specified above is encouraged; otherwise the user is advised to carefully check results.

4.2 Installing and Starting VIETUS

The VIETUS software is distributed as a compressed file (in ‘zip’ format) containing four files. The files consist of an Excel workbook file, two text files, and an electronic version of this report. These files may be extracted into any convenient directory, but all three files must be in the same directory (otherwise VIETUS will not run). Note that, when uncompressed, the three files will occupy a total of about 90 MB of hard-disk space.

To run VIETUS, simply open the Excel workbook file, as you would any other Excel workbook. It is recommended that you manage the use of the VIETUS software for different scenarios/projects by changing the VIETUS workbook file name (either by copying and renaming the original VIETUS file or by performing a “SaveAs...” operation from within Excel).

The VIETUS workbook relies on user-defined functions (i.e., macros) to perform certain calculations, so macros must be enabled for calculations to work properly. The user should select the “Enable Macros” option when opening a VIETUS workbook. If not presented with an option to enable macros, the user can try closing and re-opening the file or the user may need to alter the macro security settings within Excel. Security options in recent versions of Excel are found under the name of “Macro Security” or “Trust Center” (depending on the version of Excel). Security options can be set to prompt/notify the user to confirm whether macros should be enabled (or not) for a specific workbook.

4.3 Description of the VIETUS Workbook

The VIETUS Excel workbook contains three worksheets, including a software notice, the “HLC” worksheet, and the “VIETUS” worksheet. The software notice worksheet provides important notification/disclaimer text relevant to the use of the software. The “HLC” and “VIETUS” worksheets are described below.

The “HLC” worksheet is a repository for contaminant-specific information, including molecular weight [Wieser and Berglund, 2009], vapor pressure correlation coefficients [Yaws et al., 2009], solubility correlation coefficients [Mackay et al., 2006; Yaws et al., 2009], and correlation coefficients for the gas diffusion coefficient [Yaws et al., 2009]. The “HLC” worksheet also has data for water density as a function of temperature [HBCP, 2014], viscosity of air as a function of temperature [Lemmon, 2014], molecular weight of water [Wieser and Berglund, 2009], and the gas constant [Mohr et al., 2012]. Figure 7 shows the list of contaminants, molecular weights, correlation coefficients, and associated equations (additional annotations and data for water density/air viscosity are not shown). The user will not generally need to visit the HLC worksheet because it is simply a data repository.

Contaminant Abbrev.	Contaminant	Molecular Weight (g/mol)	Correl. Coef. for Calculating Vapor Pressure			Correlation Coefficients for Calculating Solubility						Correl. Coef. for Calculating Gas Diffusion Coef.			
			A	B	C	Equation	A	B	C	D	E	F	A	B	C
CT	Carbon Tetrachloride	153.823	7.01144	1278.54	232.888	2	9.7842 E-2	-1.4942 E-3	3.5854 E-5	2.2775 E-7	0	0	-4.1620 E-2	2.5749 E-4	5.3598 E-7
CF	Chloroform	119.378	7.11148	1232.79	230.213	2	9.9500 E-1	-1.0531 E-2	7.9819 E-5	6.6431 E-7	0	0	-4.9960 E-2	2.8829 E-4	5.9407 E-7
DCM	Dichloromethane	84.933	7.11464	1152.41	232.442	2	1.9610	-4.4883 E-2	8.6617 E-4	4.9463 E-6	0	0	-5.6860 E-2	3.3534 E-4	6.8151 E-7
CM	Chloromethane	50.488	6.99771	870.17	235.586	3	1.4019	-6.3562 E-2	1.7198 E-3	-2.8262 E-5	2.5268 E-7	-9.3470 E-10	-6.9250 E-2	4.2133 E-4	8.2225 E-7
PCE	Tetrachloroethene	165.833	7.06892	1458.45	226.986	1	2.6479 E-1	-1.5487 E-3	2.4477 E-6	0	0	0	-3.6840 E-2	2.3847 E-4	5.1123 E-7
TCE	Trichloroethene	131.388	6.87981	1157.83	202.58	1	1.4049	-8.2223 E-3	1.3218 E-5	0	0	0	-4.1270 E-2	2.6580 E-4	5.5704 E-7
1,1-DCE	1,1-Dichloroethene	96.943	7.21678	1181.12	240.84	1	6.2741	-3.8257 E-2	6.0461 E-5	0	0	0	-4.5030 E-2	2.9721 E-4	6.0085 E-7
cDCE	cis-1,2-Dichloroethene	96.943	7.21953	1290.28	236.887	1	2.7735 E+1	-1.7832 E-1	2.9328 E-4	0	0	0	-4.6220 E-2	3.0091 E-4	6.1981 E-7
tDCE	trans-1,2-Dichloroethene	96.943	7.21356	1244.35	239.497	1	7.8039	-4.5457 E-2	6.9676 E-4	0	0	0	-4.6380 E-2	3.0373 E-4	6.2044 E-7
VC	Vinyl Chloride	62.498	6.91423	911.15	239.8	4	-4.6670 E+2	1.3479 E+4	1.8523 E+2	-1.3236 E-1	0	0	-5.4240 E-2	3.6658 E-4	7.2028 E-7
1,1,1,2-TeCA	1,1,1,2-Tetrachloroethane	167.849	7.03897	1467.16	222.34	1	2.1790	-1.3966 E-3	2.9328 E-5	0	0	0	-3.6290 E-2	2.2950 E-4	4.9507 E-7
1,1,1,2-TeCA	1,1,2,2-Tetrachloroethane	167.849	6.91043	1378.88	197.086	1	4.8798	-3.0937 E-3	5.2051 E-5	0	0	0	-4.0420 E-2	2.2899 E-4	4.9882 E-7
1,1,1-TCA	1,1,1-Trichloroethane	133.404	7.00718	1253.2	229.624	1	1.0909	-6.5278 E-3	1.1075 E-5	0	0	0	-4.5040 E-2	2.5770 E-4	5.3553 E-7
1,1,2-TCA	1,1,2-Trichloroethane	133.404	7.14357	1457.65	228.099	1	2.8980	-1.8585 E-2	3.4896 E-5	0	0	0	-4.4400 E-2	2.5339 E-4	5.4055 E-7
1,1-DCA	1,1-Dichloroethane	98.959	7.18316	1269.43	237.755	1	9.4136	-5.7249 E-2	9.1784 E-5	0	0	0	-4.7450 E-2	2.8979 E-4	5.9566 E-7
1,2-DCA	1,2-Dichloroethane	98.959	7.29525	1407.85	235.48	1	1.7915 E+1	-1.1684 E-1	2.0003 E-4	0	0	0	-4.8920 E-2	2.9847 E-4	6.0315 E-7
CE	Chloroethane	64.514	7.13047	1097.6	246.009	2	5.8420 E-1	-1.6863 E-3	9.3949 E-5	-2.5316 E-6	0	0	-5.5930 E-2	3.4520 E-4	6.8934 E-7
$x = (x_p / 100) \cdot (MW_w / MW) = x_f \cdot (MW_w / MW)$ $H = [(P / 760) / x] \cdot [MW_w / (\rho_w \cdot R_{gas} \cdot T_k)]$			$\text{Log}(P_{vap}) = A - B/(T_c + C)$ Yaws et al., 2009 P_{vap} = Vapor Pressure (mm Hg)			$x_p = A + B \cdot T_k + C \cdot T_k^2$ Mackay et al., 2006 $x_p = A + B \cdot T_c + C \cdot T_c^2 + D \cdot T_c^3$ Mackay et al., 2006 $x_p = A + B \cdot T_c + C \cdot T_c^2 + D \cdot T_c^3 + E \cdot T_c^4 + F \cdot T_c^5$ Mackay et al., 2006 $\text{Log}(x_f) = A + B/T_k + C \cdot \text{Log}(T_k) + D \cdot T_k$ Yaws, 2003 x_p = mass fraction \times 100% x_f = mass fraction						$D_g = A + B \cdot T_k + C \cdot T_k^2$ Yaws, 2003 D_g = Gas Diffusion Coeff. in Air (cm ² /s)			
MW from Wieser & Berglund, 2009			Tc = Temp. in °C		Tk = Temp. in K										

Figure 7. View of the primary data (molecular weights and correlation coefficients) on the “HLC” worksheet of the VIETUS workbook

The “VIETUS” worksheet is the primary user interface, on which the user enters data and the results for the vapor intrusion estimate are displayed. Columns A:F on the “VIETUS” worksheet contain several blocks of cells for entry of input parameters, a block of cells displaying intermediate calculation results, and a block of cells for the final results, as depicted in Figure 8. By default, the “VIETUS” worksheet has space for up to three independent site scenarios (columns D, E, and F). Input parameters are segregated into several blocks (with shading in light blue hues), with each block containing related parameters. Moving from top towards the bottom, the first block contains parameters related to the nature of the source area and the vadose zone contaminant transport scenario. The second block contains primary vapor intrusion parameters that must be specified by the user. The third block contains primary vapor intrusion parameters that can either be directly specified by the user or which may be automatically calculated based on certain assumptions (discussed in Sections 0 and 2.5). The fourth block contains the secondary vapor intrusion parameters. Additional blocks of cells show the calculated intermediate values (light green shading) and concentration estimate results (tan shading).

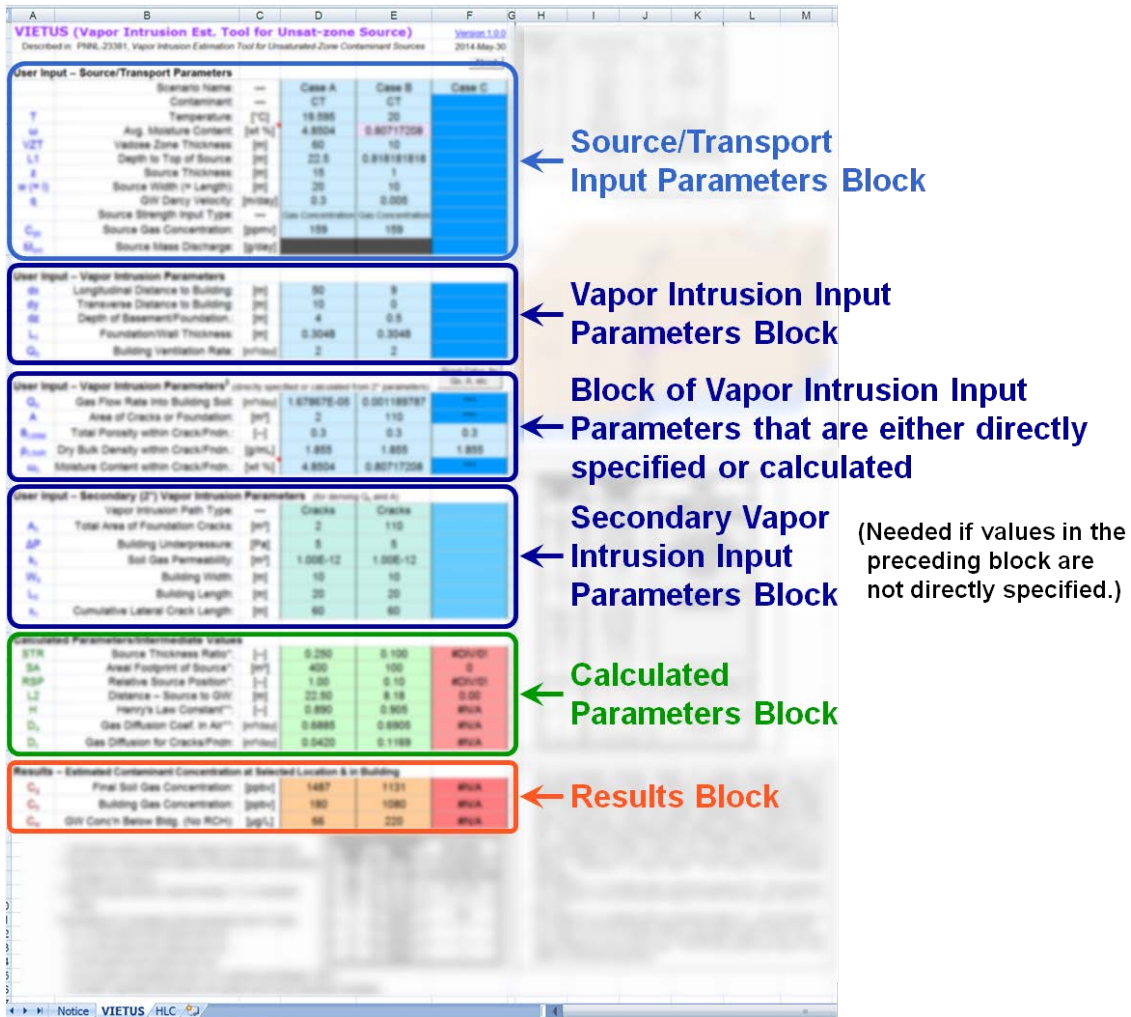


Figure 8. Groupings of worksheet cells into blocks for input parameters (blue hues), intermediate calculations (green hues), and results (tan/orange hues). The input parameters are the only items that the user will modify.

Figure 9 shows the details of the “VIETUS” worksheet, including parameter descriptions, variable names, and units of the parameters. For user convenience, additional information is presented to the right of and below the data input/calculational blocks. This additional information includes a figure representing the generalized conceptual model (to clarify the meaning of parameters) and tables/notes about the permissible ranges of parameter values. While the on-worksheet information is useful for quick reference, the user should refer to this document for details.

One additional (optional) input is present to the right (in cell L28); this input affects the range for moisture content and is discussed in Section 4.4, along with information about how to use the tool.

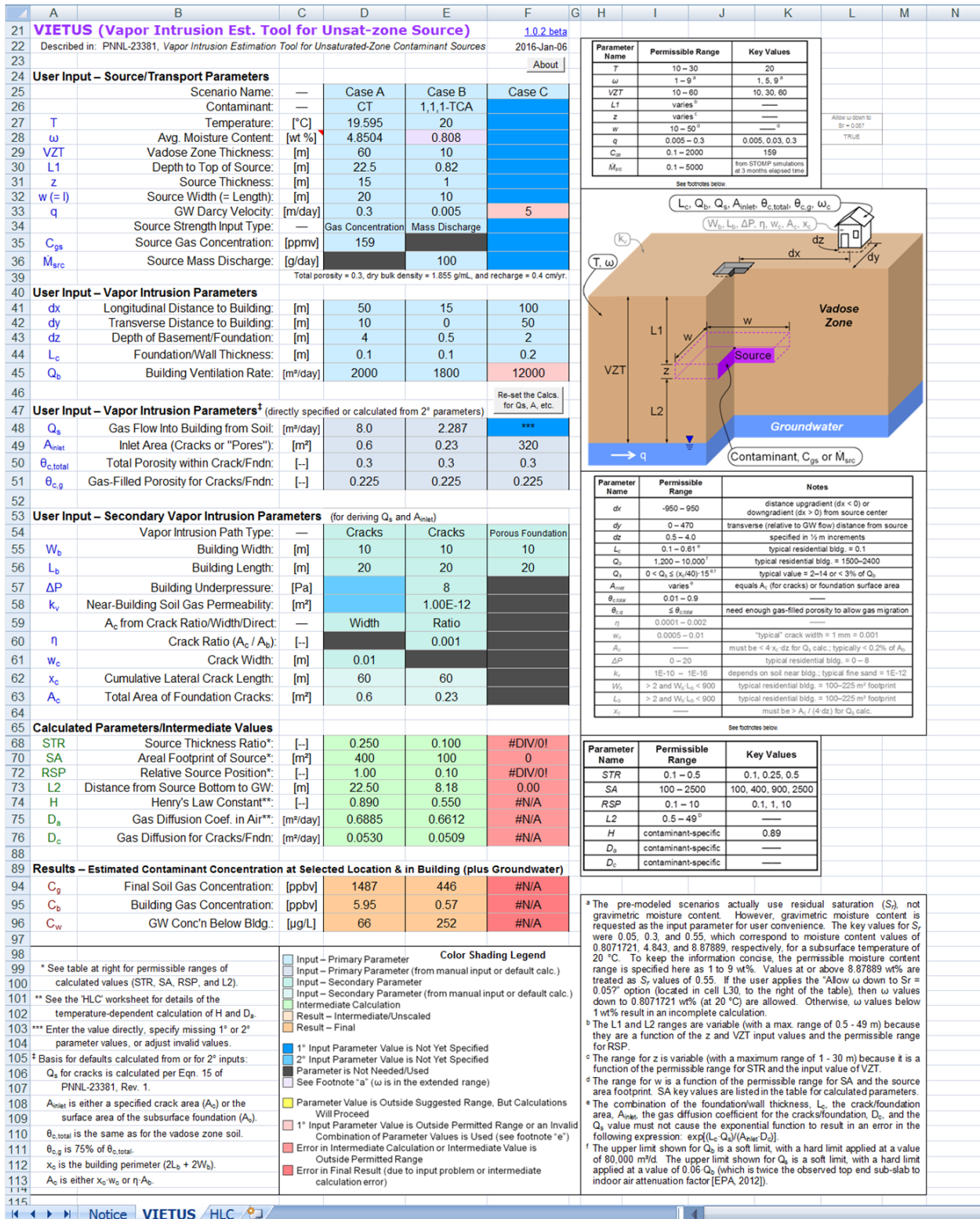


Figure 9. View of the “VIETUS” worksheet, showing details of the input parameters, intermediate calculations, results, and reference information. Scenario 3 (Test C) has little data, showing the coloration of empty cells and cells with errors (due to missing and out-of-range data).

4.4 Using the Software

The VIETUS software is implemented as an Excel workbook, thus the standard features of Excel apply. Hence, the user should be familiar with using Excel. Once a VIETUS workbook is opened (and macros are enabled, as discussed in Section 4.2), performing calculations is as simple as entering the data required to describe the site of interest using the context of the generalized conceptual site model (Section 2.1). On input of valid data, results are displayed immediately.

The VIETUS workbook includes two features to help maintain the integrity of the calculations. The associated macro code is locked for viewing or editing. In addition, the worksheets are protected and data entry is only allowed in appropriate data input cells.

For most items, data entry consists of entering parameter values for a particular scenario (in columns D, E, and/or F). Empty data input cells are all shaded a (darker) blue color, with the shading color changing upon entry of data (to either a light blue/aqua, light yellow, or light red, as shown in Figure 9). Light red shading of an input parameter value or an intermediate calculation value indicates that invalid data has been entered for one or more parameters. Light yellow shading indicates that a recommended bound has been exceeded. The primary cause of errors is likely to be data values outside the permissible ranges or values that are inconsistent with each other, such as a source thickness that is inconsistent with the vadose zone thickness and/or L1 parameter. The tables of permissible ranges and a diagram of the generalized conceptual site model are included directly on the worksheet to help the user identify issues with input data.

Selection lists are provided for the contaminant name, source strength input type, depth of basement/foundation, vapor intrusion path type inputs, and crack area calculation approach to ensure entry of valid data. A selection list is activated by selecting the input cell on the spreadsheet then clicking on the arrow button that appears. The selection of the source strength input type modifies the requested input data to be either source gas concentration or source mass discharge, while graying out the unused parameter. Similarly, the selection of a porous foundation as the vapor-intrusion path type causes the total area of foundation cracks parameter to be grayed out. Also, the selection of Ratio, Width, or Direct as the approach for estimating crack area will alter the required inputs.

An optional input (“Allow ω down to $S_r = 0.05$?”) exists in cell L28 to indicate whether soil moisture (ω) values down to the equivalent residual saturation (S_r) of 0.05 should be allowed (true) or not (false). This effectively alters the permissible range, as described in Section 2.1 (and Figure 5). Soil moisture values that are below the listed lower range and those that are above the maximum residual saturation are colored light lavender to indicate that special circumstances are in effect.

The contaminant source/transport input parameters are relatively straightforward, but the vapor intrusion input parameters encompass three blocks of related inputs, as discussed in Section 4.3. The first block consists of key parameters that must be specified by the user. The second block consists of key parameters for which a formula is provided to calculate the value (based on secondary input parameters or porous media properties). The third block consists of the optional secondary input parameters. The user has two options for setting the values of the second block of vapor intrusion input parameters. The user can enter the input parameter values directly (and leave the secondary vapor intrusion input parameters unspecified). Alternatively, the user can specify the secondary vapor intrusion input parameters and allow the second block of vapor intrusion input parameters to be calculated automatically based on the approaches and assumptions discussed in Sections 0 and 2.5. If the user directly specifies the value for a

vapor intrusion parameter in the second block and later decides to instead use the secondary input parameters to calculate that parameter, the formulas for the second block of vapor intrusion parameters can be re-set by clicking on the “Reset Calcs...” button at row 46.

The final output consists of the estimated values for the soil-gas concentration underneath the building and the contaminant concentration inside the building due to vapor intrusion. For reference, the concentration of contaminant in the groundwater directly below the specified point of interest is also shown. This groundwater concentration arises solely from the specified vadose zone source and the resulting steady state contaminant distribution. Other potential groundwater contamination (from historical and/or non-vadose zone sources) is not reflected in the groundwater concentration displayed in VIETUS. The displayed groundwater concentration is an average estimated concentration for the top meter of aquifer (which differs from SVEET [Truex et al., 2013], where groundwater concentrations are averaged over a specified well screen length). Sites with groundwater sources or with higher recharge may have different groundwater concentrations and may need a full site-specific numerical model to assess the impacts beyond the current vadose zone source.

5.0 References

- Brennan, R.A., N. Nirmalakhandan, and R.E. Speece. 1998. "Comparison of Predictive Methods for Henry's Law Coefficients of Organic Chemicals." *Water Res.*, 32(6):1901-1911.
- Chen, F., D.L. Freedman, R.W. Falta, and L.C. Murdoch. 2012. "Henry's Law Constants of Chlorinated Solvents at Elevated Temperatures." *Chemosphere*, 86(2):156-165.
- EPA. 2004. *User's Guide for Evaluating Subsurface Vapor Intrusion into Buildings*. U.S. Environmental Protection Agency, Office of Emergency and Remedial Response, Washington, D.C.
- EPA. 2012. EPA's Vapor Intrusion Database: Evaluation and Characterization of Attenuation Factors for Chlorinated Volatile Organic Compounds and Residential Buildings. EPA/530/R-10/002, U.S. Environmental Protection Agency, Office of Solid Waste and Emergency Response, Washington, D.C.
- HBCP. 2014. "Standard Density of Water." In: *CRC Handbook of Chemistry and Physics*, 94th Edition (Internet Version 2014), W. M. Haynes, ed. CRC Press/Taylor and Francis, Boca Raton, Florida.
- Johnson, P.C., and R.A. Ettinger. 1991. "Heuristic Model for Predicting the Intrusion Rate of Contaminant Vapors into Buildings." *Environ. Sci. Technol.*, 25(8):1445-1452.
- Lemmon, E.W. 2014. "Thermophysical Properties of Air." In: *CRC Handbook of Chemistry and Physics*, 94th Edition (Internet Version 2014), W. M. Haynes, ed. CRC Press/Taylor and Francis, Boca Raton, Florida.
- Mackay D, WY Shiu, K Ma, and SC Lee. 2006. *Handbook of Physical-Chemical Properties and Environmental Fate for Organic Chemicals*, Second Ed, Volume II, Halogenated Hydrocarbons. CRC Press, Boca Raton, Florida.
- Mohr, P.J., B.N. Taylor, and D.B. Newell. 2012. "CODATA Recommended Values of the Fundamental Physical Constants: 2010." *J. Phys. Chem. Ref. Data*, 41(4):043109.
- Nazaroff, W.W. 1988. "Predicting the Rate of ²²²Rn Entry from Soil into the Basement of a Dwelling Due to Pressure-Driven Air Flow." *Radiat. Prot. Dosim.*, 24(1-4):199-202.
- Oostrom, M., M.J. Truex, A.K. Rice, C.D. Johnson, K.C. Carroll, D.J. Becker, and M.A. Simon. 2014. "Estimating the Impact of Vadose Zone Sources on Groundwater to Support Performance Assessment of Soil Vapor Extraction." *Ground Water Monitoring and Remediation*, 34(2):71-84.
- Sander, R. 1999. "Modeling Atmospheric Chemistry: Interactions Between Gas-Phase Species and Liquid Cloud/Aerosol Particles." *Surv. Geophys.*, 20(1):1-31.
- Staudinger, J., and P.V. Roberts. 2001. "A Critical Compilation of Henry's Law Constant Temperature Dependence Relations for Organic Compounds in Dilute Aqueous Solutions." *Chemosphere*, 44(4):561-576.
- Truex, M.J., D.J. Becker, M.A. Simon, M. Oostrom, and A.K. Rice. 2013. *Soil Vapor Extraction System Optimization, Transition, and Closure Guidance*. PNNL-21843, Pacific Northwest National Laboratory, Richland, Washington.

- Warneck, P. 2007. "A Review of Henry's Law Coefficients for Chlorine-Containing C₁ and C₂ Hydrocarbons." *Chemosphere*, 69(3):347-361.
- White, M.D., and M. Oostrom. 2006. *STOMP Subsurface Transport Over Multiple Phases, Version 4.0, User's Guide*. PNNL-15782, Pacific Northwest National Laboratory, Richland, Washington.
- Wieser, M.E., and M. Berglund. 2009. "Atomic Weights of the Elements 2007 (IUPAC Technical Report)." *Pure Appl. Chem.*, 81(11):2131-2156.
- Yaws, C.L. 2003. *Yaws' Handbook of Thermodynamic and Physical Properties of Chemical Compounds*. Knovel, New York. Electronic ISBN 978-1-59124-444-8.
- Yaws, C.L., P.K. Narasimhan, and C. Gabbula. 2009. *Yaws' Handbook of Antoine Coefficients for Vapor Pressure (2nd Electronic Ed.)*. Knovel, New York. Electronic ISBN 978-1-59124-879-8.

Distribution

**No. of
Copies**

**No. of
Copies**

2 **Local Distribution** (*electronic*)

Pacific Northwest National Laboratory
MJ Truex K7-73
CD Johnson K7-73



Pacific Northwest
NATIONAL LABORATORY

*Proudly Operated by **Battelle** Since 1965*

902 Battelle Boulevard
P.O. Box 999
Richland, WA 99352
1-888-375-PNNL (7665)

U.S. DEPARTMENT OF
ENERGY

www.pnnl.gov